THESIS FOR THE DEGREE OF DOCTOR OF PHILOSOPHY

Voltage Stabilizers: From Design to Synthesis, Processing and Electrical Characterization

MARKUS JARVID

Division of Applied Chemistry/Polymer Technology

Department of Chemical and Biological Engineering

CHALMERS UNIVERSITY OF TECHNOLOGY

Göteborg, Sweden 2014

VOLTAGE STABILIZERS: FROM DESIGN TO SYNTHESIS, PROCESSING AND ELECTRICAL CHARACTERIZATION

MARKUS JARVID

ISBN 978-91-7597-059-2

Doktorsavhandlingar vid Chalmers tekniska högskola
Ny serie nr 3740
ISSN 0346-718X

Applied Chemistry/Polymer Technology
Department of Chemical and Biological Engineering
Chalmers University of Technology
SE-412 96 Gothenburg
Sweden
Telephone + 46 (0) 31-772 10 00

Cover, from top to bottom:
Electrical tree growing from a 10 µm diameter tungsten wire embedded in XLPE under ramped AC voltage.
Polarized optical micrographs of a grain of PCBM placed on ~10 µm thin XLPE films that were heated to 290 °C and cooled to room temperature at 20 °C min^{-1}.
Polarized optical micrographs of a grain of fullerene (C_{60}) placed on <10 µm thin XLPE films that were heated to 290 °C and cooled to room temperature at 20 °C min^{-1}.

Chalmers Reproservice
Gothenburg, Sweden 2014

Voltage Stabilizers: From Design to Synthesis, Processing and Electrical Characterization

MARKUS JARVID

Department of Chemical and Biological Engineering
Chalmers University of Technology
Gothenburg, Sweden

ABSTRACT

Voltage stabilizers are additives capable of inhibiting electrical treeing; a degradation mechanism for insulation materials subjected to strong divergent electric fields. The intended use is in cross-linked polyethylene (XLPE) high voltage power cable insulation where minute defects in the manufacturing process can give rise to the conditions needed for the initiation of treeing, which in the worst case scenario leads to failure of the insulation system with blackouts and expensive repairs as a consequence. The main purpose of this thesis is to develop a deeper understanding of the underlying mechanisms of voltage stabilization. A robust test method for the purpose of studying electrical tree initiation was developed and used throughout this thesis. This test method is further analyzed in the thesis of Anette Johansson, twin PhD collaborator in this work. A range of voltage stabilizers were evaluated in treeing experiments. Molecular modelling was used to calculate several molecular properties and clear trends were found relating the stabilizing efficacy to the electron affinity of the voltage stabilizer. An increase of more than 100% in the average onset field of electrical treeing has been achieved using a small addition of 0.33wt% of voltage stabilizer, which is also compatible with modern cross-linking methodology.

Keywords: *Polyethylene, XLPE, Electrical treeing, Voltage stabilizer, Degradation, Cable, Insulation*

LIST OF PUBLICATIONS

This thesis is based on the following scientific papers, referred to by their roman numerals in the text. The papers are appended at the end of the thesis.

Paper I. **Evaluation of the Performance of Several Object Types for Electrical Treeing Experiments**
Markus Jarvid, Anette Johansson, Jörgen Blennow, Mats R. Andersson, Stanislaw Gubanski
Dielectrics and Electrical Insulation, IEEE Transactions on, 20, 5
2013, pp*: 1712 – 1719*, DOI: 10.1109/TDEI.2013.6633701

Paper II. **Electrical tree inhibition by voltage stabilizers**
Markus Jarvid, Anette Johansson, Villgot Englund, Stanislaw Gubanski, Mats R. Andersson
Electrical Insulation and Dielectric Phenomena (CEIDP), 2012 Annual Report Conference on, Montreal, Canada, 2012, pp: 605 – 608, DOI: 10.1109/CEIDP.2012.6378853

Paper III. **Tailored Side-Chain Architecture of Benzil Voltage Stabilizers for Enhanced Dielectric Strength of Cross-Linked Polyethylene**
Markus Jarvid, Anette Johansson, Jonas Mattiasson Bjuggren, Harald Wutzel, Villgot Englund, Stanislaw Gubanski, Christian Müller, Mats R. Andersson
Journal of Polymer Science Part B: Polymer Physics, 2014, 52, pp: 1047-1054, DOI:10.1002/polb.23523

Paper IV. **A New Application Area for Fullerenes: Voltage Stabilizers for Power Cable Insulation**
Markus Jarvid, Anette Johansson, Renee Kroon, Jonas Mattiasson Bjuggren, Harald Wutzel, Villgot Englund, Stanislaw Gubanski, Mats R. Andersson, Christian Müller
Submitted Manuscript

Paper V. **Thioxanthone derivatives as stabilizers against electrical breakdown in cross-linked polyethylene for high voltage applications**

Harald Wutzel, Markus Jarvid, Jonas Bjuggren, Anette Johansson, Villgot Englund, Stanislaw Gubanski, and Mats R. Andersson

Submitted Manuscript

Paper VI. **High Electron Affinity: a Guiding Criterion for Voltage Stabilizer Design**

Markus Jarvid, Anette Johansson, Stanislaw Gubanski, Angelica Lundin, Villgot Englund, Christian Müller, Mats R. Andersson

Submitted Manuscript

Paper VII. **Analysis of Multiple Electrical Trees Incepted at Wire Electrode Test Object by Means of PD Detection**

Anette B. Johansson,Thomas Hammarström, Markus Jarvid,Stanislaw Gubanski,

Proc. of Jicable HVDC'13 Seminar, Perpignan, France, 2013, paper P06

CONTRIBUTION REPORT

Paper I. Shared main authorship with A.J. Responsibility for the material processing and design of press forms. Idea generation, sample preparation, collection and analysis of data as well as writing were done together.

Paper II. Main author. Synthesised stabilizer. Design of experiment, sample preparation, data collection and analysis as well as upgrades to the measuring setup were done together with A.J.

Paper III. Responsible for experimental design and idea generation as well as data analysis and writing. Performed SAXS measurements. Collected complementary DSC data. Performed and analysed electrical treeing measurements together with A.J. Synthesis work was shared with J.M.B and was partly supervised by H.W.

Paper IV. Main author. Responsible for all data analysis. Performed SAXS measurements. Performed electrical treeing measurements together with A.J. Sample preparation work was shared with H.W.

Paper V. Performed electrical treeing measurements together with A.J. Performed SAXS measurements. Performed and analysed DFT calculations. Shared writing with HW.

Paper VI. Main Author. Performed all experimental work and data analysis as well as DFT calculations. Electrical treeing measurements were performed together with A.J.

Paper VII. Performed sample preparation and electrical treeing measurements together with A.J.

PUBLICATIONS NOT INCLUDED IN THE THESIS

Paper VIII. **Dielectric strength of γ-radiation cross-linked, high vinyl-content polyethylene**

Andersson, M. G., Jarvid, M., Johansson, A., Gubanski, S., Foreman, M., Müller, C., Andersson, M. R.

Manuscript

Paper IX. **Influence of incorporating different electron-rich thiophene-based units on the photovoltaic properties of isoindigo-based conjugated polymers: An experimental and DFT study**

Zhuang, W., Bolognesi, M., Seri, M., Henriksson, P., Gedefaw, D., Kroon, R., Jarvid, M., Lundin, A., Wang, E., Muccini, M., Andersson, M.R.

Macromolecules, 46, 21, 2013, pp 8488-8499 DOI: 10.1021/ma401691r

Paper X. **Synthesis and characterization of benzodithiophene–isoindigo polymers for solar cells**

Ma, Z., Wang, E., Jarvid, M.E., Henriksson, P., Inganäs, O., Zhang, F., Andersson, M.R.

J. Mater. Chem., 22, 5, 2012, pp 2306-2314 DOI: 10.1039/C1JM14940G

Paper XI. **Effects of inclusions of oxidized particles in XLPE on treeing phenomena**

Doedens, E., Johansson, A., Jarvid, M., Nilsson, S., Bengtsson, M., Kjellqvist, J.

Electr. Insul. Diel. Phen. (CEIDP), 2012 An. Rep. Conf., pp 597 – 600 DOI: 10.1109/CEIDP.2012.6378851

Paper XII. **A versatile system for electrical treeing tests under AC and DC stress using wire electrodes**

Johansson, A. B. Gubanski, S., Blennow, J., Jarvid, M., Andersson, M. R., Sonerud. B., Englund, V., Farkas, A.

8th International Conference on Insulated Power Cables, Jicable'11, 2011, Versailles – France

TABLE OF CONTENTS

1 INTRODUCTION

Electrical power can be distributed via an alternating current (AC) or a direct current (DC) network. In the late 1800s, AC became the standard method for power distribution as proposed by Nikola Tesla and George Westinghouse.[1] Thomas Edison was at the time pushing for DC transmission instead but lost "the war of currents", mainly because no convenient way to change the voltage level for DC existed. For AC, this was easily done using transformers. Even though many new technologies are available today, AC power distribution involves much lower installation costs and is therefore still the standard for power distribution. DC is, however, necessary for connecting asynchronous AC grids[2] or for long-distance sub-sea transmissions[3].

The overall losses for both AC and DC transmission can be reduced by increasing the transmission voltage. This is because the main part of transmission and distribution losses is Joule losses,[4] which are proportional to the square of the current (I). By raising the voltage (V), the same power (P) can be transmitted at a lower current ($P = I * V$) and the current dependent losses can thus be decreased significantly. Improvement of transmission efficiency as well as capacity is of high priority as it is a prerequisite for realizing Europe's ambitious environmental goals.[5]

While the total energy consumption in Europe is rather constant, there is a strong trend towards electrification. The European commission predicts that an increasing fraction of the total energy consumption will be electrical energy.[5] This development is driven by political requirements, which demand increased use of renewable energy sources and also new technological platforms such as electric vehicles.[6] European goals include that by 2020, greenhouse emissions should be reduced by 20%, the energy efficiency should be increased by 20% and 20% of the total energy consumption should come from renewable energy sources compared to the level of 1990.[5] By 2050, the emission of greenhouse gasses should be reduced by 80% compared to the level of 1990.[5]

The power sector certainly has significant potential to reduce CO_2 emissions both by installation of renewable energy sources and by increasing efficiency as well as reliability of electrical transmission; an endeavor often referred to as the "smart grid" development.[7] Therefore, strong growth of renewable sources of electricity such as wind farms[8,9], solar[10-12], hydro[13] and geothermal power[14] can be anticipated in the near future together with a considerable expansion of the electrical power grid.[15]

The currently planned projects of pan-European significance in the time span between 2010 and 2020 involve about 52,300 km of new or upgraded high voltage routes (*cf.* Table 1.1), which can be compared to the existing grid length of about 305,000 km. This corresponds to investments of about € 100 billion.[16]

Table 1.1. *Currently planned high voltage routes of pan-European significance in the time span between 2010 and 2020*[16]

AC	**Distance** (km)	**DC**	**Distance** (km)
Overhead lines ≥ 220 kV	28400	Overhead lines ≥ 150 kV	2100
Inland cables >330 kV	420	Inland cables ≥ 150 kV	1490
Sub-sea cables >330 kV	400	Sub-sea cables ≥ 150 kV	9000

Installation and infrastructure that permits a higher voltage rating is, however, more cost intensive.[17] Thus, a trade-off between upfront investment cost and reduced losses has led to typical long distance transmission voltages of 400 kV or 220 kV.[16]

The quality of the insulation material that is used for a high voltage power cable can have a significant influence on the efficiency of power transmission. For AC cable insulation, improvements in dielectric strength can result in a significant increase in lifetime as well as the possibility to increase the voltage rating of a cable without change of its geometry. Cross-linked polyethylene (XLPE) is the most commonly used insulation material in high voltage cable insulation[18] and will be discussed in further detail in Chapter 3. Parameters such as microstructure[19,20] and cleanliness[21]

have been shown to be of importance with regard to dielectric strength. However, promising results have also been reported for certain additives known as "voltage stabilizers"[22,23], which when added to the polymeric insulation material increase its dielectric strength by increasing the onset of electrical treeing, an important pre-breakdown mechanism for high voltage cable insulation.

This thesis is the result of a twin PhD collaboration between the departments of Chemical and Biological Engineering/Polymer Technology, and Materials and Manufacturing Technology/High Voltage Engineering, both at Chalmers University of Technology. The project was funded by the Chalmers Area of Advance, Materials Science as well as Borealis AB who also contributed in kind. The general aim of this PhD project, the material side of the twin-project, was to improve the understanding of the underlying mechanisms for voltage stabilization of XLPE. For this purpose, XLPE materials modified with new voltage stabilizers were examined utilizing a combination of polymer characterization methods, electrical measurements and computational chemistry. The second part of the twin-PhD project, performed by Anette Johansson, aimed to develop new characterization methods that permit to monitor the initiation of electrical treeing.

2 HIGH VOLTAGE AC POWER CABLES

This chapter gives an introduction to the relevant aspects of power cable design.

2.1 High voltage power cable design

High voltage AC (HVAC) power cables are used to transmit large amounts of electrical power. An extruded high voltage power cable (*cf*. Fig. 2.1) consists of (A) a conducting core, either copper or aluminum, surrounded by several concentric layers (in contrast to conventional air-insulated overhead lines[24] which generally utilizes a naked conductor). The cable core is stranded to improve flexibility and its cross-section is directly related to the current rating of the cable. The first layer surrounding the conductor (B) is semiconducting, meaning that the electrical conductivity is modulated according to the experienced electric field. It serves to even out the electric field and to provide a void-free interface between the conductor and the insulation.[25] The semiconducting layers are typically made of carbon black filled XLPE. The next layer (C) is the insulation. The most critical parameters for the insulation material are low electrical conductivity, low dielectric losses, high dielectric strength and sufficient form stability at the operating temperature.[26] Additionally, the required lifetime, and hence long term stability, is typically around 50 years.[27] XLPE is today the most commonly used insulation material for new installations while the older oil-paper based technologies are used less frequently.[25,28] The insulation is surrounded by a second semiconducting layer followed by a conducting screen (D) which can have several purposes including giving improved mechanical strength, contributing to forming a radial field and to confine the electric field within the cable. It additionally serves as a return path for short-circuit currents, thereby avoiding these current in the soil, and it can also serve as a moisture barrier.[25] A thermoplastic outer jacket (E) for additional external protection is also necessary. Additionally, several extra layers such as mechanical protection or moisture barriers, can be included depending on the intended application, e.g. sub-sea[3] or underground cables[4].

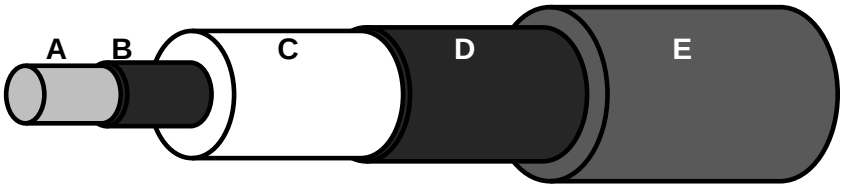

Figure 2.1. *Schematic drawing of a high voltage cable comprising (A) a central conducting core that is surrounded by (B) a semiconducting shield, (C) an insulation layer of e.g. polyethylene, (D) a semiconducting shield surrounded by a conducting screen and (E) an outer jacket.*

2.2 Characteristic impedance and transmission losses

The maximum length of an AC cable segment is limited mainly by its high capacitance, which causes a phase difference, θ, between voltage, V, and current, I. The useful active power P can be expressed as

$$P = VI\,|cos\theta| \qquad \text{Equation 2.1}$$

The remaining power is transformed into reactive power Q. This effect increases with both cable length and voltage level.[18]

$$Q = VI\,|sin\theta| \qquad \text{Equation 2.2}$$

This can be remedied by various reactive power compensation technologies.[29] Nevertheless, it is not suitable to use AC cables over distances of more than ~100 km.[18] Instead, high voltage DC (HVDC) cable technology is becoming increasingly important for long distance, especially sub-sea, transmission as DC cables do not have significant capacitive losses.

The resistive losses in the conductor are proportional to the square of the current and are transformed to heat in the cable. This is also known as Joule heating. For bulk transmission of power it is therefore preferred to use a high voltage to be able to keep current level low and in this way minimize both Joule losses and conductor size. Large cable dimensions complicate manufacture and transport and additionally result in increased material consumption which has an environmental impact on its

own.[30] It is therefore essential to have an insulation material that is able to withstand a strong electric field for operation at high voltages. A way to improve polyethylene in this regard is through the addition of voltage stabilizers, which is the focus of this thesis.

3 POLYETHYLENE

The polymerization of ethylene was discovered by accident in 1933 by Reginald Gibson and Eric Fawcett but it was not until 1935 that a reproducible synthesis procedure was developed by Michael Perrin.[31] The resulting material known as polyethylene is today the most common synthetic polymer with a worldwide annual production of around 80 million tonnes. The majority of polyethylene is used for packaging but there are numerous other applications such as household articles, pipes and cables.[32] Although the chemical structure of the polyethylene monomer is simple, its properties vary strongly with for example molecular weight and branching as well as processing conditions. This chapter aims to provide an introduction to the most relevant aspects of polyethylene with regard to this thesis.

3.1 Polyethylene synthesis

Most polyethylene grades are polymerized using transition metal catalysts of different types.[33] Most widely used are the titanium based Ziegler-Natta catalysts, for which Karl Ziegler and Giulio Natta were awarded the Nobel Prize in chemistry in 1963.[33] A wide variety of polyethylene qualities can be obtained by using α-olefin co-monomers such as hexene to induce short chain branching. Long chain branches can be induced using certain metallocene or chromium oxide catalysts.[34] The molecular weight can be controlled by increasing the amount of hydrogen in the feed, which serves as a chain length control agent in most polymerizations.[34,35] High density polyethylene (HDPE) and linear low density polyethylene (LLDPE) are examples of polyethylene grades that can be produced using Ziegler-Natta catalyst at temperatures between 80 and 95 °C at ethylene partial pressures of 0.7 to 1.5 MPa.[34]

LDPE is produced without metal catalysts at very high pressure (120-300 MPa), either in long tubular reactors or in stirred autoclaves. LDPE is characterized by a large degree of both long and short chain branching.[34,35]

The molecular structure of three major PE grades; high density polyethylene (HDPE), linear low density polyethylene (LLDPE) and low density polyethylene (LDPE), is illustrated in Fig. 3.1 together with the cross-linked version of LDPE (XLPE).

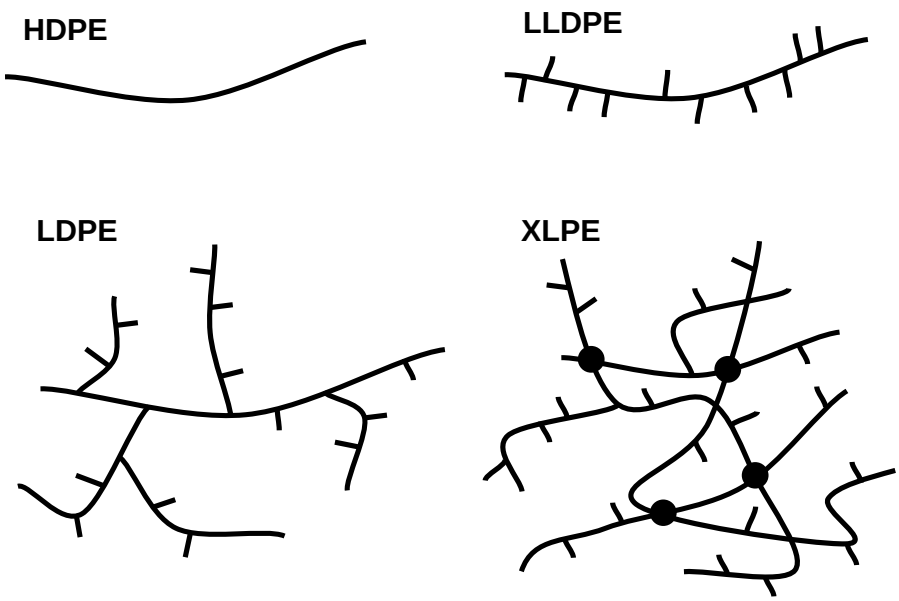

Figure 3.1. *Schematics of major polyethylene grades. Lines indicate hydrocarbon chains and intermolecular cross-links are indicated with dots.*

3.2 Microstructure of polyethylene

Important parameters determining the physical properties of polyethylene include the crystallinity and the size of the crystalline domains as well as the degree of entanglement[36] and cross-linking. In the molten state the material is liquid but as the temperature decreases the polymer chains start to order into crystalline structures with parallel crystalline sheets, so called lamellae that are separated by amorphous material as illustrated in Fig. 3.2.[37] Crystallization can be initiated either through heterogeneous nucleation e.g. from impurities or from polyethylene seed crystals or, less likely, through homogenous nucleation.[38] From the nucleation site, the crystalline domains will grow radially, forming spherulites, or axialites in the case

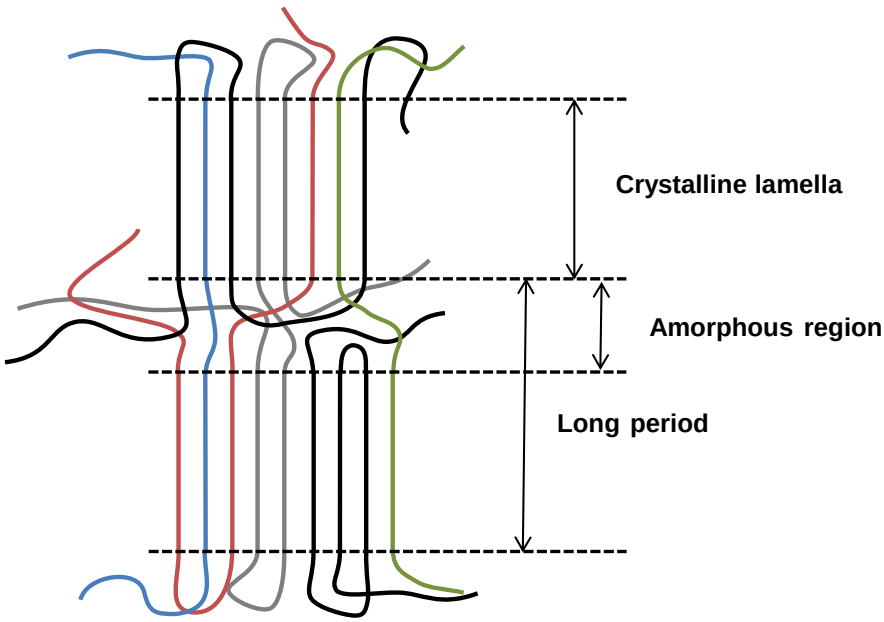

Figure 3.2. *Schematic of crystalline and amorphous regions in a semi-crystalline polymer*

of densely cross-linked polyethylene[39] where crystal growth is more restricted. The number of nucleation sites will determine the size of spherulites, which can influence for example optical clarity.[40] In Paper IV of this thesis, the change in spherulitic structure has been used as proof for solubility of an investigated stabilizer (*cf.* Fig. 3.3).

The lamellar thickness is an important microstructural parameter that for example has a strong impact on the electrical properties. The size of individual lamellae is determined in part by the chain configuration, e.g. branching, but also the thermal history of the material. Material that is not incorporated in crystals forms amorphous regions between the lamellae. The average repeat distance, composed of lamellar thickness plus thickness of the enclosed amorphous region (long period, *cf.* Fig. 3.2), can be measured using small angle X-ray scattering (SAXS).[41,42] An average value can be obtained from the associated peak in Lorentz-corrected SAXS patterns q_p (Fig. 3.4a), which corresponds to a long period $L_p = 2\pi/q_p$. The total

crystallinity X can be measured using differential scanning calorimetry (DSC). Variations in heat capacity are accounted for by adopting the total enthalpy method wherein X is calculated as

$$X = \frac{\Delta H_f}{\Delta H_f^0 - \int_{T_1}^{T_2}(C_p^{amorph} - C_p^{crystal})dT} \qquad \text{Equation 3.1}$$

where ΔH_f is the enthalpy of fusion calculated from the integrated area of the DSC melting endotherm, ΔH_f^0 ~290 J g^{-1}[38,43] is the enthalpy of fusion of 100% crystalline polyethylene and C_p^{amorph} and $C_p^{crystal}$ are the heat capacity of the amorphous and crystalline phase, respectively.[44] The product of crystallinity and long period gives the average lamellar thickness l_c according to

$$l_c = X \cdot L_p. \qquad \text{Equation 3.2}$$

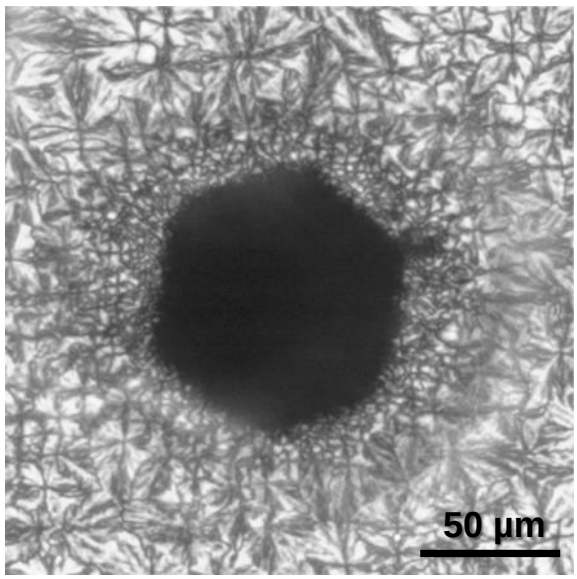

Figure 3.3. *Polarized optical micrograph of a grain of C_{60} fullerene placed on ~10 µm thick LDPE film that was heated to 300 °C and cooled to room temp. at 20 °C min^{-1} (inset: chemical structure of C_{60}). Changes in spherulitic structure around the central C_{60} crystal occurs as a result of C_{60} diffusion.*

The lamellar thickness l can be found independently using the Thompson-Gibbs equation[38]

$$l(T_m) = \frac{2\sigma_e}{\Delta H_f^0} \frac{T_m^0}{T_m^0 - T_m} \qquad \text{Equation 3.3}$$

where σ_e = 90.4 mJ m^{-2} is the fold surface energy and T_m^0 = 418.6 K denotes the equilibrium melting temperature of polyethylene.[39,45,46] As indicated by Eqn. 3.2, the melting temperature is directly related to the lamellar thickness and can thus be used to obtain the lamellar thickness distribution or peak value (*cf.* Fig. 3.4b).

The crystallization temperature (and rate) will strongly influence the lamellar thickness. At temperatures close to the crystallization temperature T_c, the polymer chain mobility is high, which promotes the growth of thick lamellae whereas thin lamellae melt. Annealing at a temperature just below the melting peak can maximize the lamellar thickness while quench-cooling from the melt will result in thinner lamellae. A DSC scan can provide useful information on for example cooling rate[47] or storage temperature[48]. The total crystallinity of polyethylene is

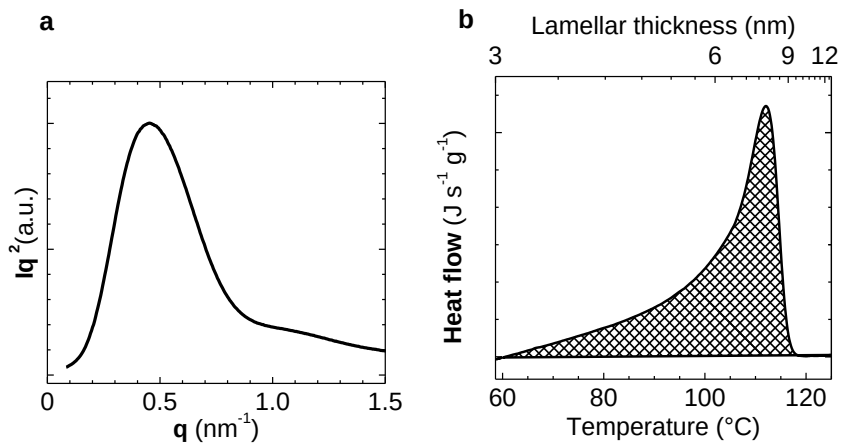

Figure 3.4. *(**a**) Lorentz-corrected small-angle X-ray scattering (SAXS) pattern of XLPE. (**b**) Differential scanning calorimetry (DSC) first heating thermogram of XLPE with corresponding lamellar thickness estimated using Eq. 3.2.*

however not influenced to the same extent by the thermal history due to the overall high rate of polyethylene crystallization.

3.3 Thermal degradation and stabilization of polyethylene

The deterioration of polymers in the presence of oxygen is a well-known phenomenon that affects material properties negatively. For polyethylene at moderate temperatures (room temperature to ~150 °C), this is conveniently described by the autoxidation cycle (*cf.* Fig. 3.5). Alkyl radicals react readily with molecular oxygen (a) to form peroxy radicals. The peroxy radical abstracts hydrogens from another polymer chain (b); this step is rate determining for the autoxidation cycle. The formed hydroxyradical can decompose into a variety of radicals, typically hydroxy and alkoxy compounds (c), which in turn form new alkyl radicals (d). Each cycle produces two new alkyl radicals that can initiate further degradation.[49,50]

For this reason, all polyethylene compounds are stabilized with antioxidants. There are several types of antioxidants that interact with different steps in the autoxidation cycle. Chain breaking acceptors (CBA) are antioxidants that scavenge primary alkyl radicals, which would in principle stop autoxidation before it starts. However, CBAs are not very effective in the presence of oxygen since the reaction rate of oxygen with primary polyethylene radicals is generally higher than that of the antioxidants. Chain breaking donors (CBD) interact instead by providing easily abstractable hydrogens to the peroxy radicals and by providing non-destructive deactivation routes for the radicals. The formed hydroperoxides can be deactivated using hydroperoxide decomposers (HD). Good stabilization against thermo-oxidative degradation can be achieved by combining several functionalities, which often results in a synergistic effect.[49,50] The antioxidant used in this thesis, 6,6'-di-tert-butyl-4,4'-thiodi-m-cresol, is such a stabilizer and is additionally known to bind covalently to the polymer matrix during peroxide cross-linking,[51] thus eliminating the risk of stabilizer migration and phase separation in the final product. This antioxidant has also been reported to nucleate LDPE.[52]

The abstraction of allyl hydrogens (situated next to a double bond) results in the formation of resonance stabilized radicals. These are therefore more reactive than e.g. alkyl hydrogens. The order of reactivity is: allyl hydrogen > benzyl and tertiary hydrogen > secondary hydrogen > primary hydrogen.[49,50] For this reason it is suitable to use a linker atom such as oxygen or nitrogen when attaching a solubilizing alkyl chain to the aromatic system of an additive to prevent degradation during processing. This is used as a design criterion for the new stabilizers presented in this thesis.

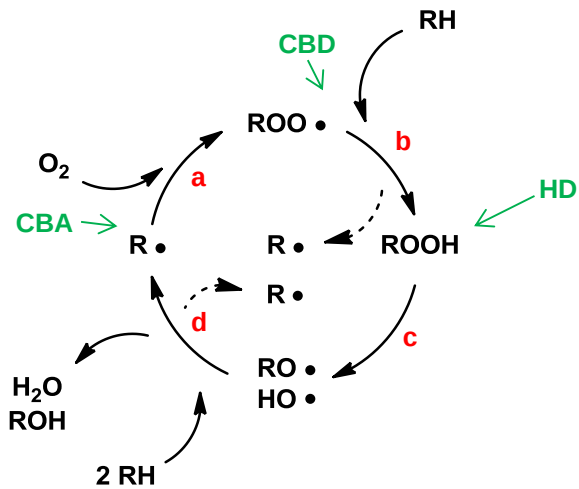

Figure 3.5. *Autooxidation cycle with chain breaking acceptor (CBA), chain breaking donor (CBD) and hydroperoxide decomposer (HD) interaction indicated. The different reaction steps a-d are discussed in the main text.*

3.4 Cross-linking chemistry

Alkyl radicals in the absence of oxygen can either lead to chain scission, disproportionation or cross-linking. Branching promotes chain scission while unsaturations, especially terminal vinyl groups, promote cross linking. For polyethylene at temperatures below 300 °C, the predominant mechanism is cross-linking[53] while in polypropylene, the predominant mechanism is chain scission.[54] Alkyl radicals can be produced in several ways. Most commonly, peroxides are used that decompose at a temperature above the melting temperature and below the

onset of material degradation so that the material can be melt processed without gel formation and cross-linked without material deterioration. For the cross-linking of LDPE for cable insulation, dicumyl peroxide (DCP)[26,55] is commonly used. During the decomposition of DCP, by-products e.g. acetophenone, cumyl alcohol and methane[56,57] (*cf.* Fig. 3.6) are formed. These by-products need to be degassed from the cable insulation both for ensuring good insulation quality as well as a good working environment. By-product removal is a time consuming process of high relevance for the output and response time of cable manufacture.[56] Radicals can also be produced using ionizing radiation, in which case the main by-product is hydrogen gas.[55,58] Cross-linking can also be achieved by introducing for example silanes on the main polymer chain that form cross links in the presence of water.[59,60] Cross-linked polyethylene displays improved thermal form stability and better resistance to environmental stress-cracking compared to non-cross linked polyethylene.[55,61] Any voltage stabilizers present during the cross-linking process should not react with the radicals to form inactive products or sublime/evaporate during degassing.

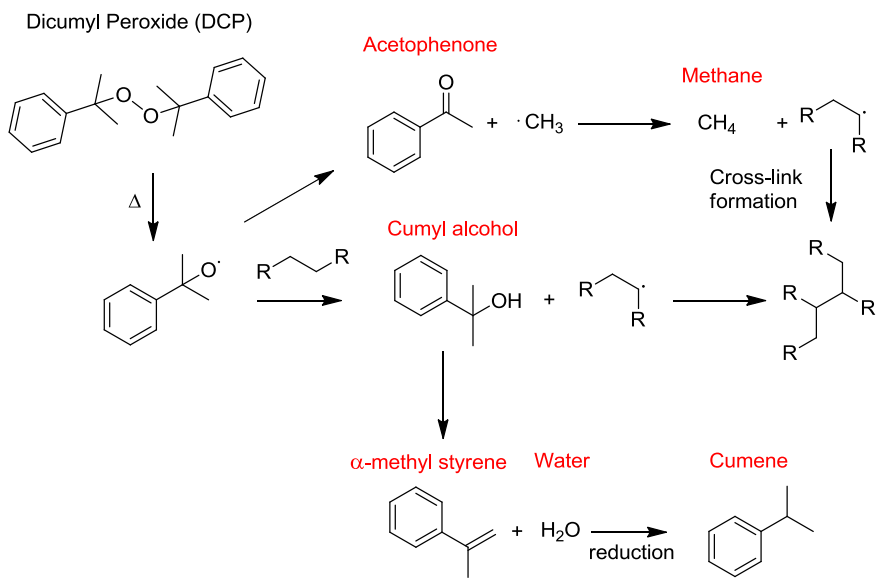

Figure 3.6. *Dicumyl peroxide (DCP) decomposition and polyethylene cross-linking mechanism[62] with unwanted by-products indicated with red labels.*

4 ELECTRICAL TREEING

High voltage cable insulation is subjected to many types of stress during its operational lifetime, which is commonly around 50 years.[27] These include thermal, mechanical, electrical, electromechanical and electrochemical stress. This can initiate several degradation processes, such as water treeing[63], stress cracking[64] and electrical treeing; the latter being a common failure mechanism that will be discussed in further detail in this chapter.

4.1 Background and theory

The first observations regarding electrical treeing were published in 1958[65] and many cable failures have been associated with this phenomenon since. An electrical tree is a gas filled, tree-like structure caused by electron avalanche erosion from partial discharges in a solid insulation material (*cf.* Fig. 4.1). The process of electrical treeing can be divided into three different stages: Initiation, propagation and breakdown and is often preceded by an inception stage.[66]

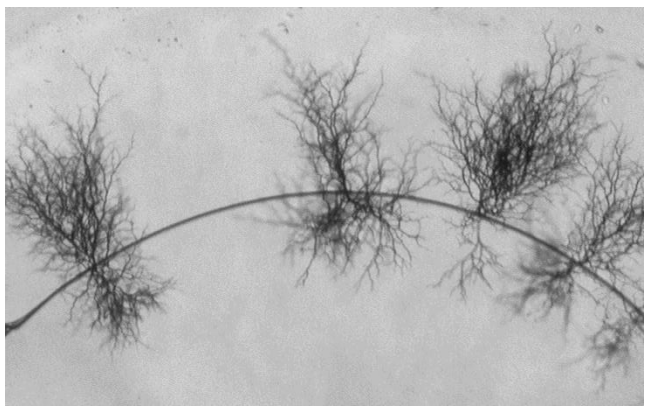

Figure 4.1. *Electrical treeing in XLPE from a ⌀=10 µm tungsten wire electrode*

Inception is the degradation process resulting in a material void large enough to sustain partial discharges. This takes place at points of strongly divergent electric field above a threshold field for electron injection. Tree inception is likely a combination of several mechanisms but the dominating mechanism is considered to

be degradation by electron impact.[67-69] Common points of origin for tree inception include organic or inorganic contaminants such as metal particles, catalyst residue or scorch[70,71] (prematurely cross-linked and oxidized material in extrusion equipment causing inhomogenities and miscoloration) or protrusions from the semiconducting layer. The tip of a water tree branch can also act as an initiation point.[72,73]

The initiation of treeing requires a region with low dielectric strength, which is able to sustain partial discharges at the local electric field level. This is typically a gas-filled void that is either a result of the inception stage or a bubble produced during material processing, e.g. a void formed due to gaseous cross-linking by-products. Once partial discharge takes place, the cavity walls quickly erode and the tree is initiated.[74]

An electrical tree will, once initiated, propagate in the general direction of the electric field. Depending on the field strength, field divergence and the insulating material, the tree can develop into different shapes and sizes, ranging from short, dense bush-type trees to long branched ones.[75] It is common that the propagation proceeds into a runaway stage where the growth rate increases rapidly. This occurs as the electrical tree branches approach the counter electrode.[74]

4.2 Evaluation of wire objects for electrical tree initiation tests

The standard method for controlled initiation of electrical trees is the double needle method.[76] Huuva et al.[77] developed an alternative test method based on a wire-plane geometry and real-time optical visualisation of the treeing process. The wire-plane test object geometry was further developed in the presented twin-PhD work (*cf.* Papers I and II) and compared with the one used by Huuva et al. as well as the standard double-needle geometry. The three test object geometries are presented in Fig. 4.2. and their properties are summarized in Table 4.1.

For the purpose of comparing electrical tree resistance in newly developed insulation materials, the wire-plane method was found to be suitable both for

practical reasons, such as material cost and time consumption, but also for the possibility of sampling relatively large material volumes in each test object.

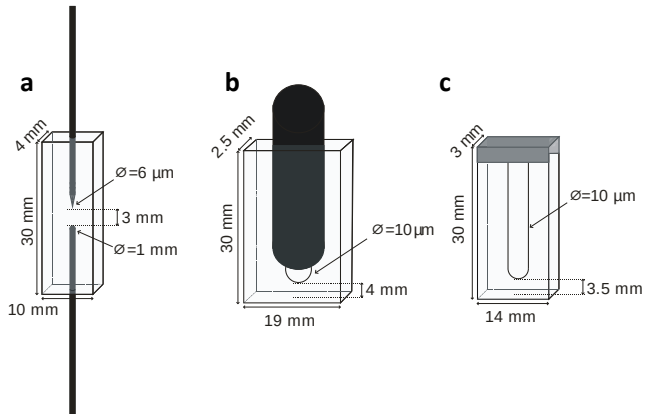

Figure 4.2. *Needle test object, standardized test method* ***(a)****, wire test object with semiconducting tab scaffold, Huuva, Englund et al.*[77] ***(b)*** *and wire test object without semiconducting tab, Jarvid, Johansson et al.*[78,79] ***(c).***

Table 4.1. *Characteristic properties of the discussed electrode geometries for electrical tree initiation*

Sharp needle	Wire – plane (Huuva, Englund et al.)	Wire – plane (Jarvid, Johansson et al.)
• Measures only one point of the material	• Weakest point of relatively large material volume measured	• Weakest point of relatively large volume measured
• Tip radius is difficult to control and is easily damaged	• Wire radius is easy to control	• Wire radius is easy to control
• Insertion of needles can cause material strain	• Microstructure around electrode less affected	• Microstructure around electrode less affected
• One tree formed	• One tree per sample used	• Multiple trees forming independently
• Strongest field enhancement	• Electrode geometry (wire loop) difficult to control	• Good control over wire-loop shape
• Standardized test method [15]		• Few test objects needed for reliable statistical analysis

4.3 Electrical tree initiation test experimental section

All data on electrical tree initiation in the following chapters have been consistently measured using the method described here.

4.3.1 Polymer material

Cross-linkable LDPE with the trade name Borlink™ LS4201S, containing dicumyl peroxide and the antioxidant 6,6'-di-tert-butyl-4,4'- thiodi-m-cresol, was obtained from Borealis AB. This LDPE is characterized by a typical melt-flow index ~ 2 g/10 min at 190 °C and 2.16 kg and density ~0.922 g cm^{-3}. The chosen LDPE grade has a low level of contaminants that may influence electrical measurements and is recommended for use in high voltage applications up to 220 kV in accordance with Boström et al.[21]

4.3.2 Test object preparation

The cross-linkable LDPE was hot-pressed at 130 °C to form two separate parts (*cf.* Fig. 4.3a), which were molded together to enclose a 10 µm diameter straightened and electrolytically cleaned tungsten wire purchased from Luma Metall. The wire works as the high voltage electrode and was fastened using aluminum tape. This was followed by cross-linking of the LDPE at 180 °C to form the final test object displayed in Fig. 4.2c and Fig. 4.3b. Cross-linking by-products were removed by degassing samples in vacuum (0.1 mbar) at 80 °C for 4 days. To ensure a comparable thermal history, cross-linked and degassed samples were re-molten at 130 °C followed by cooling to room temperature at between 0.5 and 0.2 °C min^{-1} in the temperature interval 100-60 °C. A thermocouple was used to record the cooling curve to establish that all sets of treeing test objects experienced a similar heat treatment, which was carried out immediately prior to electrical testing. DSC and SAXS were used to obtain detailed information on the resulting polyethylene microstructure. The procedures for adding voltage stabilizers are described in Section 5.6.

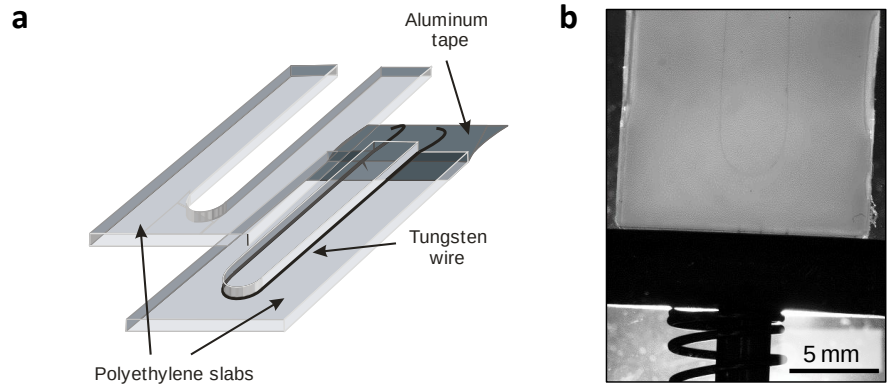

Figure 4.3. *(**a**) Exploded view drawing of the wire test object (**b**) micrograph of test object mounted for electrical treeing test with the tungsten wire loop barely visible.*

4.3.3 Test circuit, test conditions and electrical tree detection

The treeing process was observed using a stereomicroscope equipped with a CCD camera, recording the treeing process at two frames per second at a resolution of 2048 x 1532 pixels. This allowed for detection of trees smaller than 10 µm. The electrical tree initiation tests were performed in transformer oil in a custom made container, as shown in Fig. 4.4a. An electrical test arrangement as shown in Fig. 4.4b was used to supply and measure voltage as well as electrical partial discharge events taking place inside the tree channels. Detection of partial discharges is an alternative to optical detection in the case of non-transparent test objects, (*cf.* Paper VII)**.**

4.3.4 Electric field calculations

3D numerical simulations of the electric field distribution in the wire object were performed by means of finite element based software, Comsol Multiphysics.[80] The field enhancement factor K was found to be 21 mm^{-1} at the wire electrode. The maximum electric field E_{max} is thus calculated from the measured voltage U as:

$$E_{max} = KU \qquad \text{Equation 4.1}$$

See Paper I for further details.

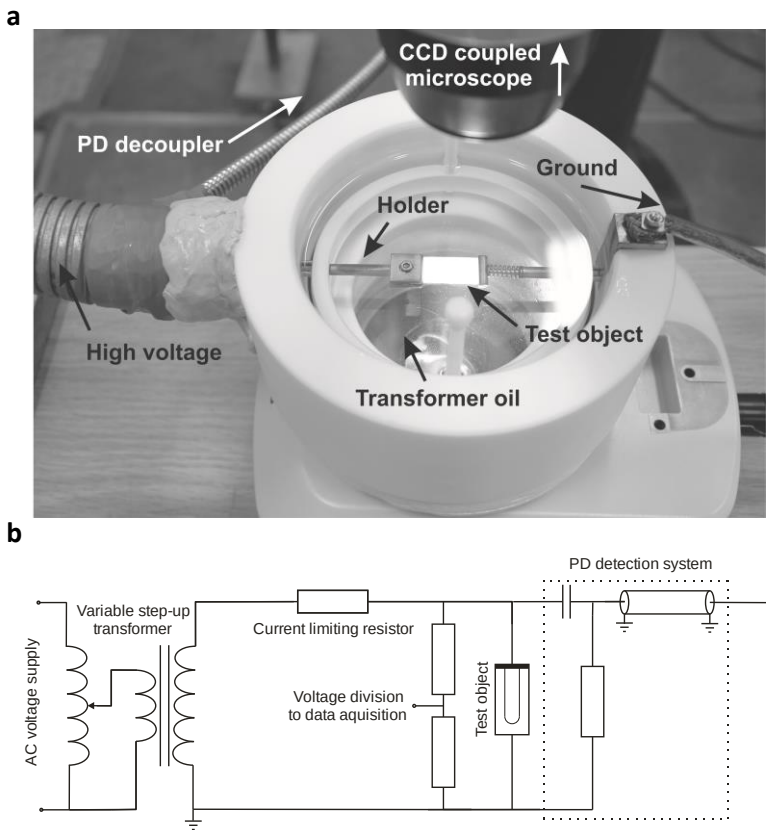

Figure 4.4. *(**a**) oil container, sample holder and high voltage/ground connections for the electrical treeing tests and (**b**) schematic of the electrical test arrangement*

4.4 Statistical analysis of treeing data

Due to the stochastic nature of electrical tree initiation it is important to perform a thorough statistical analysis of the initiation data. Tree initiation data do not normally comply with the Gaussian distribution. Instead, the Weibull distribution is recommended by several industrial standards[76,81] and has been found suitable for the data sets generated in this work.

The 3-parameter cumulative Weibull distribution function describes a set of independent statistical events such as electrical tree formation according to:

$$F(E_{tree}) = 1 - exp\left[-\left(\frac{E_{tree} - E_0}{\eta}\right)^{\beta}\right] \qquad \text{Equation 4.1}$$

where E_{tree} is the electric field, at which the onset of tree formation is observed, and β, E_0 and η are fit parameters. The fit parameters can be extracted by linearizing equation 4.1:

$$ln\left[ln\frac{1}{1 - F(E_{tree})}\right] = \beta ln(E_{tree} - E_0) - \beta ln\eta \qquad \text{Equation 4.2}$$

Figure 4.5a shows a linearized Weibull plot of the distribution for XLPE. Evidently, the data set follows a linear trend for which a high coefficient of determination $R^2 \sim 0.99$ is found, which further justifies the use of Weibull analysis for the breakdown data presented in this work.

The physical meaning of the shape parameter β is most apparent from plots of the Weibull probability density function (*pdf*) displayed in Figure 4.5b:

$$f(E_{tree}) = \frac{\beta}{\eta} \cdot \left(\frac{E_{tree} - E_0}{\eta}\right)^{\beta-1} \cdot exp\left[-\left(\frac{E_{tree} - E_0}{\eta}\right)^{\beta}\right] \qquad \text{Equation 4.3}$$

A value of $\beta > 1$ indicates that the likelihood of failure is increasing with electric field. A shape parameter of $\beta < 2.7$ or $\beta > 3.7$ indicates a *pdf* with a tail towards the right or the left of the peak probability, respectively (note that the *pdf* for XLPE in Fig. 4.5b has a tail to the right as indicated by the corresponding $\beta = 1.6$).

The electric field, at which 63% of all observed electrical trees have initiated, is given by $E_{63} = \eta + E_0$. This parameter is analogous to the mean of a normal distribution and is used to evaluate the efficiency of the new voltage stabilizers in this work. For XLPE we observed that E_{63} ~296 kV mm^{-1}, which is indicated with a dashed line in Fig. 4.5c.

The parameter E_0 represents a threshold electric field below which no electrical tree formation is observed under the employed measurement conditions. For the XLPE distribution in Fig. 4.5, the threshold value was found to be 248 kV mm^{-1}.

Electrical tree initiation tests have been performed for several independently prepared sets of reference XLPE samples as shown in Table 4.2. XLPE sample sets 2, 4, 6 and 7 were prepared using the same method. Set 1 had a slightly different thermal history (a slightly different cooling rate was used for pre-testing heat treatment) and set 5 was shown to have significantly lower gel content compared to the other sample sets (~73% instead of 78-82%). All sample sets except for set 3 is prepared from LDPE powder which has been impregnated in dichloromethane prior to test object preparation following the general procedure for addition of voltage stabilizers (*cf.* Section 5.6). The standard deviation of the E_{63} parameter for the seven sample sets (~21 kV mm^{-1}) can be used as an indication of the error of the test method. The corresponding value weighted for the total number of data points in each series was found to be ~14 kV mm^{-1}. The dataset from sample set 4 is used for comparison with stabilized materials and as error, 21 kV mm^{-1} has been used in conjunction with the E_{63} parameter.

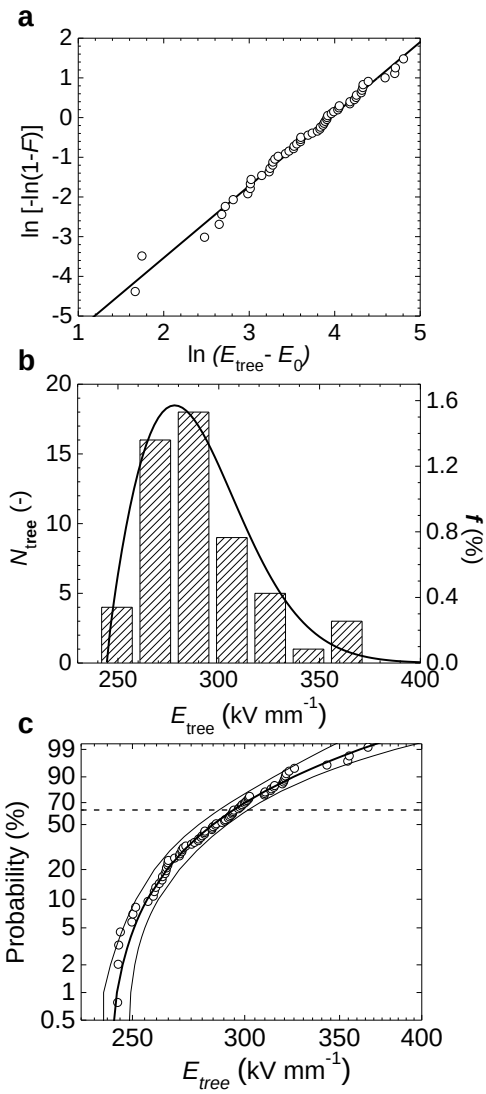

Figure 4.5. *(**a**) Linearized 3-parameter cumulative Weibull distribution describing the number of electrical tree-initiation events as a function of electric field for XLPE. A linear fit with a coefficient of determination R^2 ~0.99 indicates that Weibull statistics are obeyed. (**b**) Corresponding 3-parameter Weibull probability density function (pdf), $f(E_{tree})$, of XLPE and as well as number of tree initiations, N_{tree}, observed for different electric fields. (**c**) 3-parameter cumulative Weibull distribution function, $F(E_{tree})$, of XLPE with 95% confidence intervals indicated. The 63.2% probability is marked with a dashed line.*

Table 4.2. *3-parameter Weibull statistics for seven independent XLPE sample sets together with number of data points N*

	N (-)	E_0 (kV mm^{-1})	E_{63} (kV mm^{-1})	β (-)
XLPE batch 1	32	231	277	1.5
XLPE batch 2	20	209	301	6.3
XLPE batch 3	8	259	295	2,8
XLPE batch 4	56	248	296	1.6
XLPE batch 5	12	269	331	1.7
XLPE batch 6	24	218	291	2.8
XLPE batch 7	12	238	265	3.0

5 DESIGN, SYNTHESIS AND CHARACTERIZATION OF NEW VOLTAGE STABILIZERS

This chapter presents a summary of the work performed on synthesis and characterization of voltage stabilized materials.

5.1 Background

The concept of voltage stabilizers first appeared around the mid-1960s in a series of patents by Simplex Wire & Cable Company, featuring nitrated aromatic structures, polycyclic aromatic hydrocarbons (PAH)[82] or halogenated aromatics[83] as additives in power cable insulation. These additives were claimed to stabilize against insulation faults (electrical treeing) caused by high voltage. It was also common practice to use mixtures of stabilizers and aromatic oils, which were claimed to give the same benefits without increasing the dielectric constant or power factor of the insulation material, which occurs due to phase separation of voltage stabilizers at high loadings. At the time, only empirical observations regarding voltage stabilizers had been established.

In 1978 the first systematic study on the topic was published[22] where a series of aromatic hydrocarbons ranging from naphthalene to pyrene in size were tested. It was found that the molar voltage stabilizing efficiency correlated with the ionization energy as well as the electron affinity of the voltage stabilizers. Although this trend was not obeyed by all voltage stabilizers outside the group of aromatic hydrocarbons, the most efficient stabilizers nevertheless comprised electron donor-acceptor functionality and usually also a transferrable proton, which could move between donor and acceptor moieties, such as in e.g. 2-nitro diphenylamine, 2-nitroaniline or 2-nitrotoluene.[84] Electron donor-acceptor functionality here refers to a molecule having electron accepting and electron withdrawing groups connected through a conjugated system.

Despite promising results indicating increased electrical tree initiation voltage levels in the range of 200% compared to reference polyethylene, the voltage stabilized materials did not have commercial success. This is not surprising since the best voltage stabilizers at the time, e.g. 2-nitro diphenylamine, became inactive after cross-linking and degassing, likely as a result of degradation upon reaction with radicals. In 1976, it was shown that by modifying pyrene with a short alkyl chain, long-term stabilization of XLPE could be achieved.[85] This was followed up by a patent in 2004 by Martinotto et al.[86], who derived voltage stabilizers from acetophenone and benzophenone modified with alkyl chains. These voltage stabilizers retained their function in cross-linked and degassed materials. This idea was further developed by Englund et al.[23,87] who synthesized new benzophenone derivatives with strongly electron donating alkyl amine groups as well as rigid aromatics with the same type of chemistry. They found through the use of molecular modeling in conjunction with electrical tree initiation tests that both, benzophenone stabilizers and stabilizers based on rigid aromatic cores, exhibit a logarithmic correlation between stabilizing effect and decrease in ionization energy.

The development of voltage stabilizers in this thesis takes its start with the evaluation of benzil-based compounds; a logical step after acetophenone and benzophenone voltage stabilizers as has been reported in the recent literature.[23,86]

5.2 Benzil type voltage stabilizers: Influence of ageing, concentration and chemical modification

Seven benzil derivatives that carry alkyl chains linked to the conjugated core via ether (Et), ester (Es) or amine (Am) groups were synthesized and tested (*cf.* Fig. 5.1), full details are available in Paper III. Additionally the influence of alkyl chain length was investigated in a test series where methoxy, dodecyloxy and triacontyloxy groups were attached to the benzil core as indicated in the molecule names, e.g. Et_1, Et_{12}, Et_{30}. The use of straight alkyl chains facilitates purification of the chemicals by recrystallization. Am_1 and Benzil were purchased from TCI and Sigma Aldrich respectively. With the anticipation that ionization potential governs the efficiency of benzil stabilizers in line with the behavior of benzophenones, the

electron donating groups were put in para position to maximize their effect on the HOMO energy level.[88] Moreover, 4,4'-bis-dodecyloxybenzil (Et_{12}) was used as a model stabilizer in this thesis and has been used for additional studies such as the influence of the voltage ramp rate during electrical testing in Paper II as well as concentration and ageing on the electrical tree initiation field described by the Weibull parameters E_0, η and β (*cf.* Chapter 4). Non-modified benzil did not remain in the XLPE after degassing and was for that reason excluded from this study. This is explained by the low onset temperature of weight loss observed with thermogravimetric analysis (TGA) as shown in Table 5.1.

Table 5.1. *Melting point, T_m, and 1% TGA weight loss for benzil stabilizers*

Voltage stabilizer	T_m (°C)	**TGA, 1% weight loss** (°C)
benzil	95	133
Et_1	132	192
Et_{12}	63	305
Et_{30}	102	229
Es_2	83	194
Es_{12}	72	275
Am_1	200	277
Am_8	40	200

It was found that the E_{63} value for XLPE stabilized with benzil derivates at a concentration of 10 mmol kg^{-1} varied between 331 and 513 kV mm^{-1} depending on the pendant group of the benzil stabilizers (*cf.* Table 5.2). In this regard, the ester and amine containing stabilizers were the most efficient. There is a strong correlation between alkyl chain length and the E_{63} parameter indicating that short alkyl chains are beneficial. Although all benzil derivates increased the E_{63} value compared to XLPE, this was not the case with the E_0 parameter. With regards to the E_0 parameter, the intermediate alkyl chain length performed better; especially Am_8

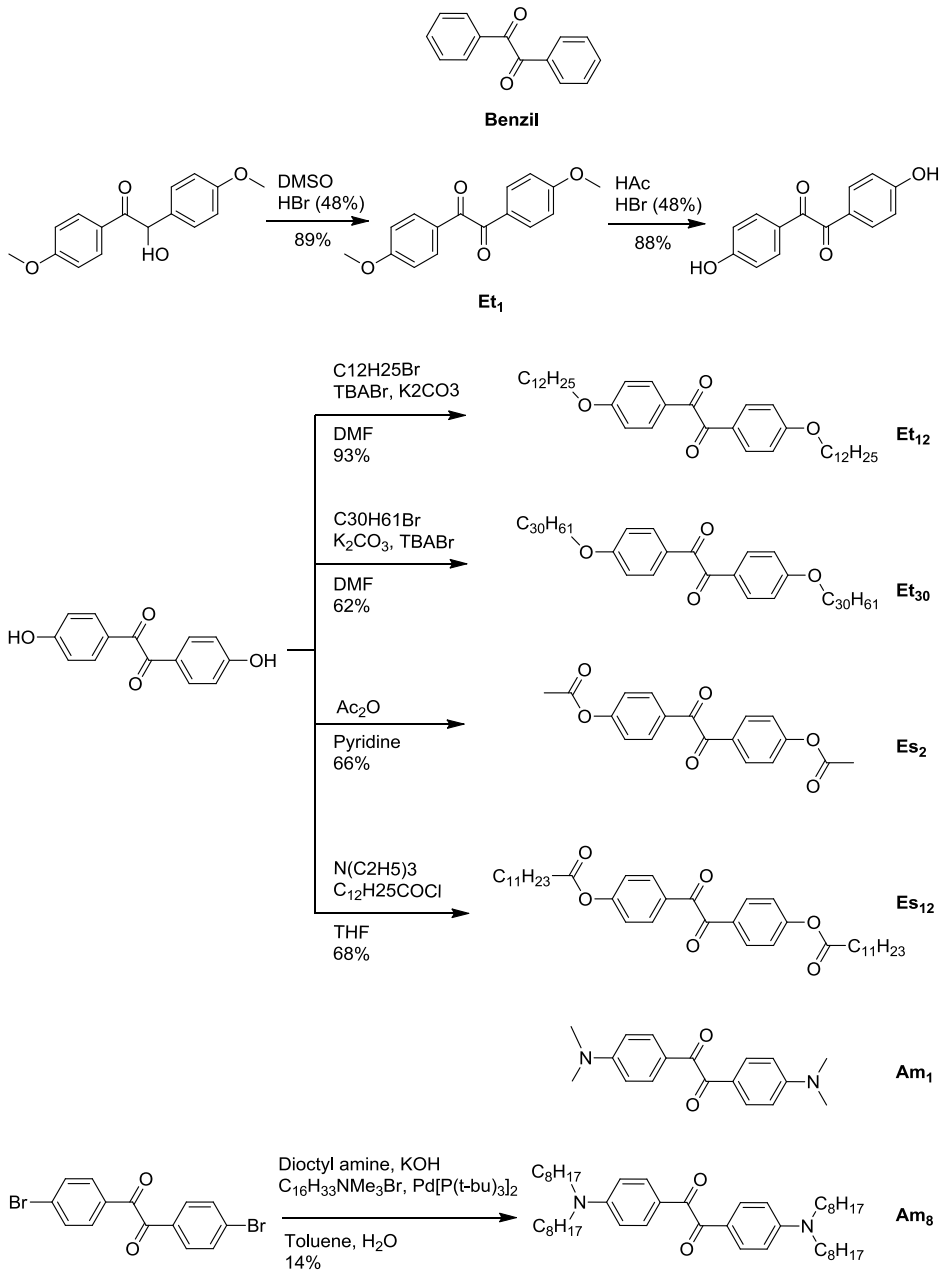

Figure 5.1. *Structures and synthesis of benzil type voltage stabilizers.*

(E_0~386 kV mm^{-1}), which also features the lowest melting point. Am_1, which has the highest E_{63} parameter, actually has the lowest E_0 value and also the highest melting point in the series (*cf.* Table 5.1). It is reasonable to assume that this correlation arises due to insufficient compatibility although no inhomogeneity was observed at the tested concentration, 10 mmol kg^{-1} (any stabilizer aggregates of size $> \sim 1$ µm would be detected optically). Also, it seems that the data sets might not always be sufficient to accurately predict the E_0 parameter as their size are sometimes touching the limit of what is recommended (≥20 are recommended by IEEE).[76]

Table 5.2. *Weibull fit parameters for electrical treeing measurements of benzil type voltage stabilizers. Number of trees included in the analysis N, threshold electric field E_0, electric field at which 63% of all samples have failed, $E_{63} = \eta + E_0$, and shape parameter β.*

Benzils	$\boldsymbol{N}$ (-)	$\boldsymbol{E_0}$ (kV mm^{-1})	$\boldsymbol{E_{63}}$ (kV mm^{-1})	$\boldsymbol{\beta}$ (-)
XLPE	56	248	296	2.1
Et_1	32	232	425	5.3
Et_{12}	60	289	376	1.8
Et_{30}	20	278	331	2.6
Es_2	20	263	509	4.0
Es_{12}	28	181	400	5.0
Am_1	28	0	513	7.3
Am_8	24	386	448	2.0

Et_{12} was the first benzil derivate that displayed a promising voltage stabilizing effect during the course of this thesis work. Even though several stabilizers with higher efficiency have been tested since, Et_{12} was used for test method development as well as investigations into the influence of concentration and ageing time on stabilizer performance (*cf.* Fig. 5.2 and 5.3). Et_{12} stabilized test objects were prepared with four additive concentrations: 10, 20, 30 and 40 mmol kg^{-1}. Electrical treeing tests were carried out according to the method presented in Chapter 4, i.e.

the measurements were performed within 24 h after sample preparation. An increase can be observed in the E_{63} value going from 10 to 20 mmol kg^{-1} reaching a rather constant value which remains similar for 30 and 40 mmol kg^{-1}. The E_0 parameter did instead decrease upon increasing the concentration. The remaining, non-tested, samples of the four above mentioned sets as well as a reference XLPE sample batch were stored at ambient temperature wrapped in aluminum foil during ~85 days after which the reference and two of the stabilized batches (10 and 20 mmol kg^{-1}) were measured again and it was found that while the reference material remained relatively unchanged, the stabilized materials seemed to have an improved performance. The E_{63}value of the 10 mmol kg^{-1} batch increased from 376 to 468 kV mm^{-1}. After a total ageing time of ~130 days the four stabilized materials were measured one final time and it could be seen that both increased E_{63} and E_0 values were obtained for all stabilized data sets except for the 10 mmol kg^{-1} batch where the E_0 value instead decreased.

Upon this relatively long term storage of the samples, a non-transparent layer developed on the surface of the test objects, especially for 20 mmol kg^{-1} and higher concentrations as a result of phase separation at sample/air interfaces indicating a solubility limit lower than 20 mmol kg^{-1} at room temperature for Et_{12}. It is therefore concluded that increasing the concentration above the room temperature solubility limit does not impair the long term stabilizing effect when using this stabilizer. In fact, the highest E_0 values were in this study obtained for the highest concentration and longest ageing time. These results emphasize the need for controlling sample storage time in a comparative study.

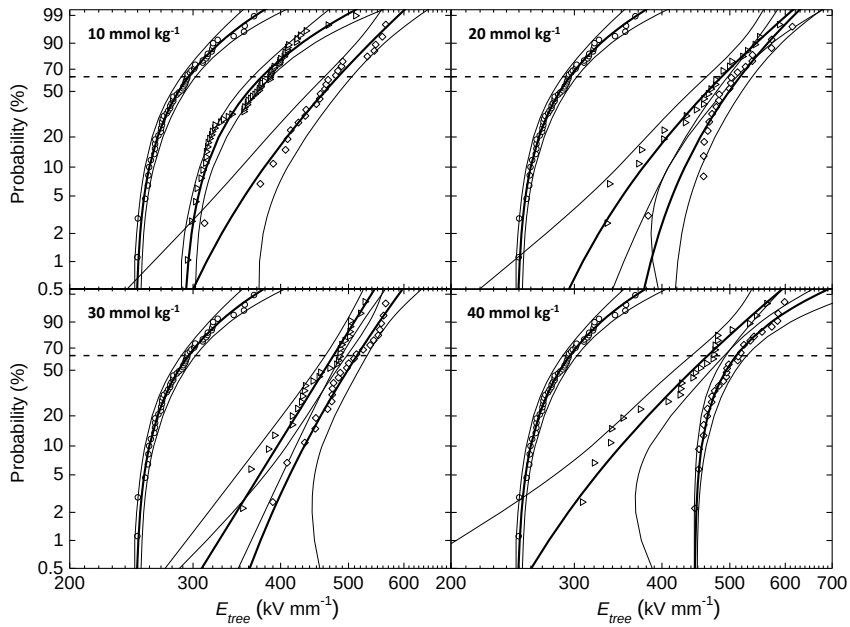

Figure 5.2. *3-parameter cumulative Weibull distribution function, $F(E_{tree})$ describing tree-initiation events as a function of electric field for XLPE with and without addition of Et_{12} at 10, 20, 30 and 40 mmol kg^{-1} concentration. Circles indicate reference XLPE while triangles and diamonds indicate XLPE voltage stabilized with Et_{12} and aged at room temperature for ~1 day or ~130 days respectively. The 63.2% probability is indicated with a dashed line.*

The same experiment was performed with 10 mmol kg^{-1} Es_2, which have a significantly higher E_{63} value from the start. Also for this system, both E_{63} and E_0 increase with ageing time (*cf.* Fig. 5.3). A possible explanations for this behavior is that as the secondary crystallization proceeds in the XLPE, the stabilizer is expelled from the crystalline domains and enriched in surrounding low density material where treeing is most likely to initiate. The stabilizer would have time to fill up voids and to distribute homogenously in the amorphous material. A second explanation is that the benzil stabilizers slowly form small aggregates with beneficial electronic properties. This could for example promote a quenching mechanism that provides a faster route for relaxation to the ground state for excited stabilizer molecules or it could be intermolecular interactions such as dipole or pi-

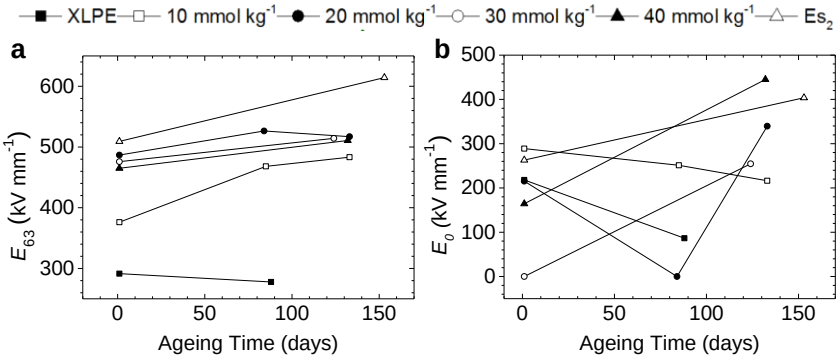

Figure 5.3. *The E_{63}* ***(a)*** *and E_0* ***(b)*** *Weibull parameters as a function of ageing time for XLPE amd various concentrations of Et_{12} as well as 10 mmol kg^{-1} Es_2.*

stacking that stabilize the charged radicals, thereby making the stabilizers more efficient according to the voltage stabilizing mechanisms discussed in Section 6.2 of this thesis.

5.3 Thioxanthone type voltage stabilizers

Thioxanthone derivates were considered as potential voltage stabilizers due to structural similarities as compared to benzophenones and benzils. Just as benzils and benzophenones, thioxanthones are efficient photosensitizers[89] and it was hypothesized that these voltage stabilizers could have a similar voltage stabilizing effect if the mechanism of tree initiation can be related to impact excitation. If this holds true, it is likely that the efficiency and stability of the voltage stabilizers can be related to the lifetime of excited states. Thioxanthones are frequently used in photopolymerization reactions for coating and inkjet applications and their photophysical properties have been investigated thoroughly. Thus, detailed data on excited state lifetime and quenching rates can be found in literature[90]. The tested thioxanthone derivatives and their synthesis are presented in Fig. 5.4 (*cf.* Paper V for full details).

Table 5.3. *Weibull fit parameters for electrical treeing measurements of thioxanthone type voltage stabilizers. Number of trees included in the analysis N, threshold electric field E_0, electric field at which 63% of all samples have failed, $E_{63} = \eta + E_0$, and shape parameter β.*

Thioxanthones	N (-)	E_0 (kV mm^{-1})	E_{63} (kV mm^{-1})	β (-)
XLPE	56	248	296	2.1
ITX	28	296	385	3.0
MeOTX	28	39	362	7.4
HOTX	24	283	410	2.6
OTXAc	28	314	404	1.3
OTXMa	22	98	459	9.3

XLPE stabilized with thioxanthone derivates at a concentration of 10 mmol kg^{-1} displayed E_{63} and E_0 parameters ranging from 362 to 459 and 39 to 314 kV mm^{-1}, respectively (*cf.* Table 5.3). Overall, the thioxanthone voltage stabilizers are not as efficient voltage stabilizers as the benzil derivates. Their efficiencies do, however, show an interesting correlation with lifetime of excited states (*cf.* Paper V).

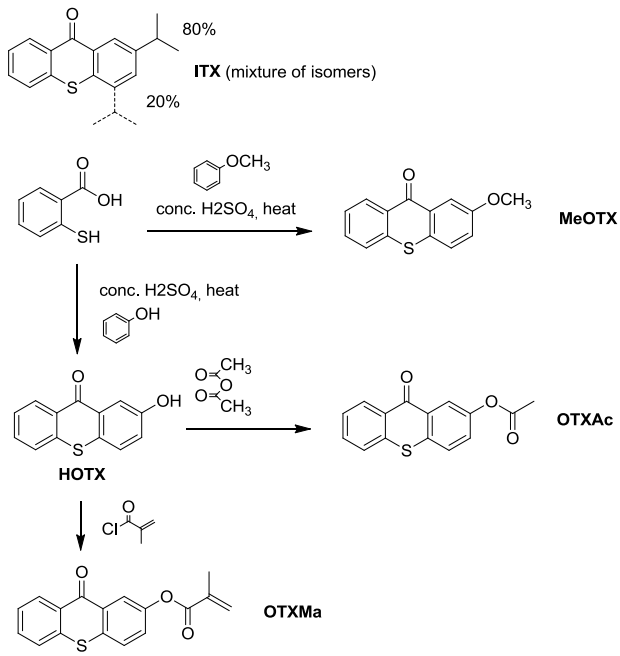

Figure 5.4. *Structures and synthesis of thioxanthone type voltage stabilizers.*

5.4 Fullerene type voltage stabilizers

From previous research on fused polycyclic aromatic systems it is logical to assume that fullerenes should act as very efficient voltage stabilizers, provided that they can be sufficiently dispersed in polyethylene. The low migration tendency of these large molecules is an additional benefit. Therefore C_{60} fullerene[91] and its solubilized derivative phenyl-C_{61}-butyric acid methyl ester (PCBM)[92] (*cf.* Fig. 5.5) were investigated as potential voltage stabilizing candidates (*cf.* Paper IV for full details). Solubility of PCBM and C_{60} in XLPE is demonstrated by visualizing its migration in a thin film of XLPE at elevated temperature (290 °C). The cross-polarized optical micrographs in Fig. 5.6 show how the size of PE spherulites changes along the concentration gradient extending radially from the central fullerene grain due to diffusion.

Fullerenes performed extraordinarily well in this study. They consistently gave rise to increased E_{63} and E_0 values compared to reference XLPE at very low molal concentrations. The best result was obtained for diffusion loaded PCBM (*cf.* Section 5.6) where E_{63}~304 and E_0~391 kV mm^{-1} using only 0.5 mmol kg^{-1}, an increase of 23% and 32% in the E_0 and E_{63} parameters respectively (*cf.* Table 5.4). In a control experiment, PCBM was also shown to be effective in the non-cross linked LDPE compound (containing DCP and antioxidant), which has a significantly higher tree initiation level compared to the XLPE used as reference material in this study (*cf.* Table 5.4). The reason for the increased tree initiation level of LDPE as compared to that observed for the XLPE compound was not investigated. However, it is likely related to the additive composition (peroxide and antioxidant and possibly minor amounts of peroxide decomposition products). Overall, PCBM was shown to be more efficient than C_{60} (*cf.* Table 5.4).

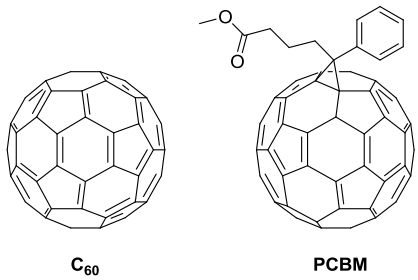

Figure 5.5. *Chemical structures of C_{60} and PCBM*

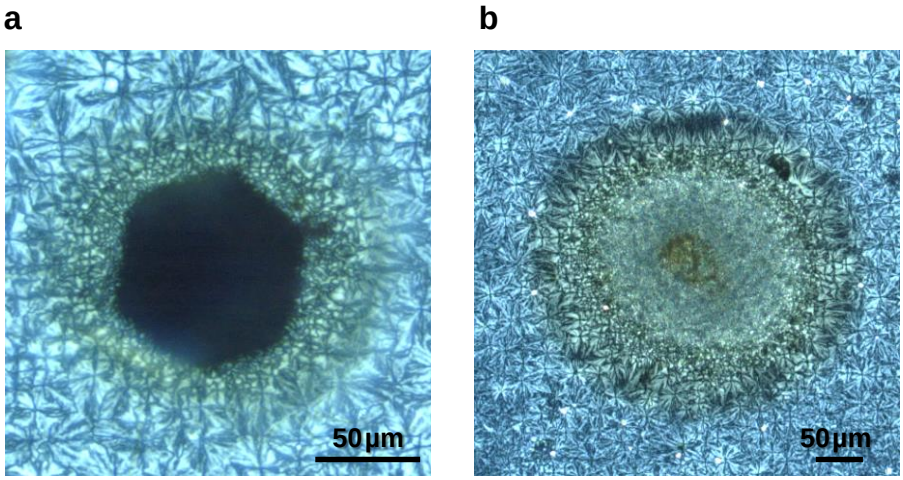

Figure 5.6. *Polarized optical micrographs of a grain of C_{60}* ***(a)*** *and PCBM* ***(b)*** *placed on ~10 µm thin XLPE films that were heated to 290 °C and cooled to room temperature at 20 °C min^{-1}.*

Table 5.4. *Weibull fit parameters for electrical treeing measurements for fullerene type voltage stabilizers. Number of trees included in the analysis N, threshold electric field E_0, electric field at which 63% of all samples have failed, $E_{63} = \eta + E_0$, and shape parameter β.*

Fullerenes	N (-)	E_0 (kV mm^{-1})	E_{63} (kV mm^{-1})	β (-)
XLPE	56	248	296	2.1
LDPE**	20	0	516	14.0
C_{60}[a]	28	257	340	2.2
PCBM[a]	20	280	372	2.2
PCBM*[b]	16	304	391	1.9
LDPE+PCBM**[a]	20	465	573	3.0

* Diffusion loaded samples
** Crosslinkable LDPE used as base resin
[a]concentration ~1 mmol/kg
[b]concentration ~0.5 mmol/kg

5.5 Additional compounds of interest

Treeing experiments on XLPE voltage-stabilized with several additional voltage stabilizers are presented here. All stabilizers are tested at a concentration of 10 mmol kg^{-1} except where stated otherwise. Anthracene and N,N'-dioctyl-4-aminobenzophenone (DOABP) act as references to the work of other authors[22,23,93].

Phenyl-amine based structures including two triazine derivates (*cf.* Fig. 5.7) were investigated due to their relatively low ionization potentials. Two triazine based compounds were synthesized where the first, Triazine 1, was composed of a 1,3,5-triazine core with three N,N-dioctylamine moieties in positions 2, 4, and 6. One of the dioctylamine moieties was exchanged for an N,N-bis(4-(tert-butyl)phenyl)amine moiety to form Triazine 2. Triazine 1 was the only compound in this thesis that significantly reduced the E_{63} parameter compared to XLPE (*cf.* Table 5.5). Triazine 2 had an E_{63} value equivalent to that of the reference.

To compare with literature values of stabilizer performance, two well performing stabilizers from previous studies were evaluated. The first was anthracene[22,93],

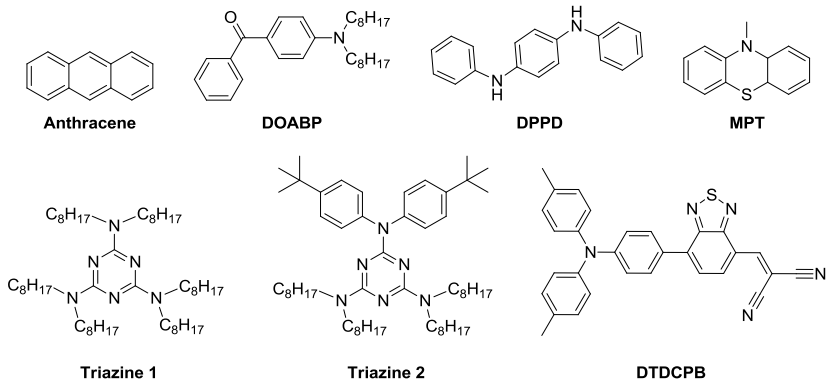

Figure 5.7. *Chemical structure and naming of voltage stabilizers.*

which at first gave rise to a tree initiation level similar to the XLPE material (*cf.* Table 5.5) and it was concluded that the anthracene evaporated during degassing of the test objects. Diffusion loaded samples (Anthracene*) showed, however, an increased voltage stabilizing effect with E_{63} ~421 and E_0 ~337 kV mm^{-1}, which reaches the performance of at least some of the benzil and thioxanthone derivates. The different methods for adding voltage stabilizer are described in Section 5.6. The second stabilizer tested for comparative purposes was N,N'-dioctyl-4-amino benzophenone (DOABP, *cf.* Fig. 5.7), [23] for which E_{63} ~341 and E_0 ~271 (*cf.* Table 5.5).

Methylated phenothiazine (MPT) (*cf.* Fig. 5.7) was tested as a comparison with the thioxanthones to investigate the effect of exchanging the electron withdrawing carbonyl moiety with an electron donating methylamine. MPT yielded values of E_{63} ~340 kV mm^{-1} (*cf.* Table 5.5), which is lower compared to those obtained with all tested thioxanthone derivates.

N,N'-diphenyl-p-phenylenediamine (DPPD) (*cf.* Fig. 5.7) was tested and yielded E_{63} ~322 kV mm^{-1}. DPPD displayed a strong color change from yellow to orange upon crosslinking and had likely been degraded. The reaction of DPPD with radicals during cross-linking is corroborated by a low gel content of ~72% (*cf.* Table 5.7).

The trends observed through DFT modeling (*cf.* Chapter 6) of the voltage stabilizers previously tested as a part of this thesis led to the testing of a compound abbreviated DTDCPB (cf. Fig. 5.7). It was anticipated to give rise to particularly promising voltage stabilizing properties due to its high electron affinity and small E_{HOMO}-E_{LUMO} difference. DTDCPB was originally designed for use in organic solar cells.[94] DTDCPB performed extraordinarily well and 9 out of 20 data points were right censored in the statistical analysis since the maximum output voltage of the electrical test setup was reached at 680 kV mm^{-1}. The E_{63} value for XLPE voltage stabilized with DTDCPB was estimated to ~734 kV mm^{-1}, an increase of 148% compared to the reference XLPE (*cf.* Fig. 5.8 and Table 5.5). DTDCPB degrades during cross-linking (as indicated by color change from blue to yellow), which is why diffusion loading (*cf.* Section 5.6) was used as an alternative means of compounding for this substance. It should be noted that visible phase separation occurred in these samples indicating a room temperature solubility <10 mmol kg^{-1} in XLPE.

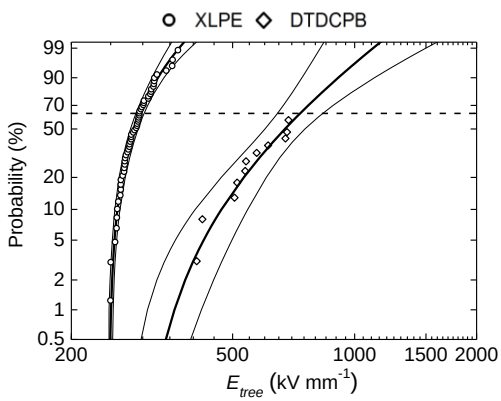

Figure 5.8. *3-parameter cumulative Weibull distribution function, $F(E_{tree})$ describing tree-initiation events as a function of electric field showing DTDCPB as compared to reference XLPE with 90% confidence intervals. The 63.2% probability is indicated with a dashed line.*

Table 5.5. *Weibull fit parameters for electrical treeing measurements. Number of trees included in the analysis N, threshold electric field E_0, electric field at which 63% of all samples have failed, $E_{63} = \eta + E_0$, and shape parameter β.*

Additional Compounds	N (-)	E_0 (kV mm^{-1})	E_{63} (kV mm^{-1})	β (-)
XLPE	56	248	296	2.1
Anthracene	16	256	289	1.3
Anthracene*	31	337	421	1.2
DOABP	32	271	341	2.7
Triazine 1	28	254	273	1.5
Triazine 2	16	0	293	20.1
DPPD	28	242	322	2.7
MPT	24	219	340	2.3
DTDCPB	20**	289	734	2.5

* Diffusion loaded samples
**9 out of 20 tree initiations right censored at 680 kV mm^{-1}

5.6 Preparation of voltage stabilized polyethylene

The main sample preparation procedure used throughout this thesis involves a solvent impregnation technique where the voltage stabilizer is dissolved in dichloromethane, which is subsequently used for impregnating LDPE powder, which already contained the peroxide and antioxidant system needed for cross-linking. The test object preparation was carried out as described in Section 4 after evaporation of the solvent. The powder was obtained by grinding liquid-nitrogen cooled LDPE pellets in a Retch grinder with a 500 µm sieve.

In three different cases another procedure was exercised, previously referred to as diffusion loaded. The stabilizer was deposited on XLPE test objects prepared as described in Section 4.3.2, followed by thermal annealing until test objects with a homogenous appearance were obtained through diffusion. In the case of anthracene, this was done at 130 °C in a sealed glass container. DTDCPB, with a melting point of ~290 °C, required a higher annealing temperature and longer annealing time. A

gradual increase in temperature up to 180 °C was sufficient. This was done during a total of 9 days in a tubular oven with continuous nitrogen flow. Similarly, PCBM was added by annealing at 180 °C for 7 days under nitrogen flow. FTIR and UV-vis was used to confirm that the stabilizers had not degraded.

5.7 Influence of degassing by-products

The voltage stabilizing effect of the DCP decomposition products, mainly acetophenone, is well known and usually gives rise to an increased tree initiation voltage of roughly 100%[22,95]. This effect diminishes as these volatile byproducts evaporate. The effect of byproducts was investigated here by omitting the degassing step for a set of reference samples. For good comparability, a heat treatment was performed in the same manner as for the other materials. During the heat treatment, these samples were put in a sealed aluminum bag to minimize the loss of byproducts. An E_{63} value of 682 kV mm^{-1} was obtained for the non-degassed material. A set of samples where the heat treatment step was omitted is included for reference in Table 5.6.

Table 5.6. *Weibull fit parameters for electrical treeing measurements for XLPE with and without DCP decomposition by-products as well as heat-treatment. Number of trees included in the analysis N, threshold electric field E_0, electric field at which 63% of all samples have failed, $E_{63} = \eta + E_0$, and shape parameter β.*

PE / XLPE	N (-)	E_0 (kV mm^{-1})	E_{63} (kV mm^{-1})	β (-)
XLPE	56	248	296	2.1
XLPE (non-heat treated)	12	239	265	3.0
XLPE (non-degassed)	28*	137	682	3.7

*9 out of 28 tree initiations right censored at 701 kV mm^{-1}

5.8 Influence on microstructure and gel content

The microstructure of polyethylene has a strong impact on electrical tree initiation. For instance, Yan *et al.* observed a linear correlation between lamellar thickness and tree initiation voltage and found that a decrease in lamellar thickness from 15 to 10 nm lowers the tree initiation voltage of non-cross linked polyethylenes, including LDPE and HDPE, by about 50%.[19,20] Takahashi *et al.* have reported a similar trend for XLPE.[96] In this thesis, DSC was used to estimate the crystallinity X of XLPE with and without voltage stabilizer according to the total enthalpy method, as described in Chapter 3.[38]

For XLPE a crystallinity of X ~56% was observed, which decreased only slightly upon addition of 10 mmol kg^{-1} of any investigated voltage stabilizer. Moreover, the peak melting temperature was found to be T_m~112 °C for neat XLPE. The Gibbs-Thomson equation was applied to estimate the peak lamellar thickness l_{peak} ~7.8 nm. This parameter also decreased slightly for the voltage stabilized materials. Additionally, the lamellar thickness was independently obtained from SAXS measurements. Lorentz-corrected SAXS patterns of all investigated XLPE materials reveal a characteristic scattering signal with a peak at q_p ~0.45 nm^{-1} (*cf.* Fig. 3.4a), which corresponds to a long period L_p~14 nm. A lamellar thickness of $l_c\left(= X * L_p\right)$ ~7.8 nm was found for XLPE. Since a decrease in crystallinity was observed for the stabilized materials, a slight decrease in lamellar thickness could be confirmed.

The maximum change in lamellar thickness resulting from the addition of any investigated voltage stabilizer was merely 1.3 nm (*cf.* Table 5.7), which according to previous literature should result in a decrease in tree initiation voltage of about 10%.[19,20] Thus, we conclude that any increase in dielectric strength is not caused by changes in polyethylene microstructure.

The degree of cross-linking was measured in terms of the gel content *G*, *i.e.* the amount of insoluble, cross-linked material that remains after careful extraction of the soluble polyethylene fraction in decahydronaphthalene, as described in Paper

III. For the majority of the tested voltage stabilizers in this thesis, the changes in gel content compared to the reference material lies within the margin of error. In a few cases, however, increased gel content was observed. This was the case for OTXMa, PCBM and, especially, C_{60} where *G* was increased to 84%, 85% and 86% respectively, which can be compared to 78-82% for reference XLPE. This is not entirely surprising as these compounds are well known to react with radicals. For instance, Krusic *et al.* have shown that methyl radicals can readily add to C_{60}[97] and Brois *et al.* have patented the use of fullerenes as cross-linking agents for saturated polymers, which in the presence of free radical initiators covalently attach to the fullerene cage.[98] OTXMa contains a methacrylate group, which is well known for its radical reactivity and is used to make acrylate polymers. The covalent bonding of voltage stabilizers to the polymer matrix is a promising aspect that eliminates the risk for additive migration and phase separation. In contrast to the use of alkyl chain chemistry, this method does not involve any risk for phase separation. For XLPE stabilized with DPPD, a significant decrease to 72% gel content was observed compared to reference XLPE, indicating stabilizer interference in the cross-linking reaction.

Table 5.7 *Physical properties of reference and voltage-stabilized XLPE (stabilizers were added before cross-linking). Crystallinity X and peak lamellar thickness l_{peak} from DSC melting thermograms, as well as average lamellar thickness $l_c = L_p * X$, where L_p ~13.7 nm is the long period obtained from SAXS measurements. G corresponds to the gel content of XLPE.*

Benzils	***X*** (%)	$\boldsymbol{l_{peak}}$ (nm)	$\boldsymbol{l_c}$ (nm)	***G*** (%)
Et_1	49	7.4	6.7	78
Et_{12}	47	7.7	6.4	80
Et_{30}	53	7.3	7.3	80
Es_2	52	7.5	7.1	80
Es_{12}	50	7.6	6.9	81
Am_1	55	7.6	7.5	78
Am_8	49	7.6	6.7	80
Thioxanthones	***X*** (%)	$\boldsymbol{l_{peak}}$ (nm)	$\boldsymbol{l_c}$ (nm)	***G*** (%)
ITX	59	7.2	8.0	81
MeOTX	47	7.5	6.4	81
HOTX	50	7.7	-	81
OTXAc	51	7.4	7.1	82
OTXMa	52	7.8	-	84
Fullerenes	***X*** (%)	$\boldsymbol{l_{peak}}$ (nm)	$\boldsymbol{l_c}$ (nm)	***G*** (%)
C_{60} [a]	55	7.3	7.7	86
PCBM [a]	52	7.2	7.2	85
Other Compounds	***X*** (%)	$\boldsymbol{l_{peak}}$ (nm)	$\boldsymbol{l_c}$ (nm)	***G*** (%)
XLPE	56	7.8	7.7	78-82
MPT	47	7.6	6.5	80
DPPD	-	-	-	72
Triazine 1	-	-	-	79
Triazine 2	-	-	-	79

[a]concentration ~1 mmol/kg

6 MOLECULAR PROPERTIES AND MECHANISMS OF VOLTAGE STABILIZATION

This chapter aims to give an overview of the mechanisms of voltage stabilization reported in the literature in the light of new trends observed by means of molecular modeling performed as a part of this thesis.

6.1 DFT calculated molecular properties of voltage stabilizers

Ab initio calculations were performed for the tested voltage stabilizers to find molecular properties related to voltage stabilizing effect. Vertical and adiabatic electron affinities and ionization potentials along with highest occupied molecular orbital energy (E_{HOMO}) and lowest unoccupied molecular orbital energy (E_{LUMO}) have been obtained using Gaussian 09[99], DFT B3LYP/6-311+G(d,p)[100-102]. Vertical (v) and adiabatic (a) ionization potential IP and Electron affinity EA are defined as:

$$IP_v = E^+(M) - E(M) \approx -E_{HOMO}$$
$$IP_a = E^+(M^+) - E(M)$$
$$EA_v = E(M) - E^-(M) \approx -E_{LUMO}$$
$$EA_a = E(M) - E^-(M^-)$$

Where E(M) represents the neutral ground state while $E^+(M)$ and $E^-(M)$ represent the cation and anion with ground state geometry. $E^+(M^+)$ and $E^-(M^-)$ represent the cation and the anion with optimized geometry. Vertical indicates that the geometry is optimized for the ground state for both neutral and charged species while adiabatic refers to the case where the geometries have been optimized for both the neutral and the charged state. The energy levels are further illustrated in Fig. 6.1 and the calculated values for the voltage stabilizers presented in this thesis are summarized in Table 6.1. All calculated molecular energies are enthalpy corrected for 298 K and 1 atm.

E_{HOMO} and E_{LUMO} indicate the highest occupied molecular orbital and the lowest unoccupied (virtual) molecular orbital energies for the system in its neutral ground state and are according to Koopmans theorem approximately equal to $-IP_v$ and $-EA_v$ respectively, although a substantial offset of ~1 eV exists. Such correlations and further experimental verification can be found in Paper VI.

The increase in electrical tree initiation field obtained when incorporating voltage stabilizers in XLPE can be described by the parameter Φ

$$\Phi = \frac{(E_{63} - E_{63}^{XLPE})}{E_{63}^{XLPE}} * \frac{1}{c} \qquad \text{Equation 6.1}$$

where E_{63} and E_{63}^{XLPE} are the 63% probability percentiles from the Weibull distribution fitted to the electrical tree initiation data sets of stabilized and reference XLPE respectively and c is the molal concentration of the stabilizer.

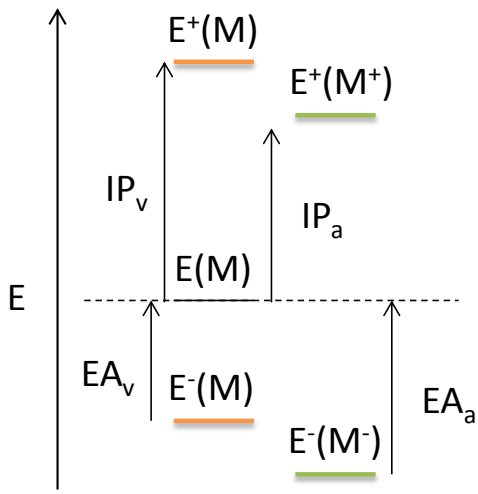

Figure 6.1. *Adiabatic ionization potential IP_a, vertical ionization potential IP_v, Adiabatic electron affinity EA_a, and vertical electron affinity EA_v visualized using molecular energies. E(M) represents the ground state while $E^+(M)$ and $E^-(M)$ represent the cation and anion with ground state geometry. $E^+(M^+)$ and $E^-(M^-)$ represent the cation and the anion with optimized (relaxed) geometry.*

In Fig. 6.2, the calculated molecular properties were correlated with Φ for the stabilizers presented in this thesis as indicated using red circles. The adiabatic ionization potentials and electron affinities have been used in this plot but the same trends are seen when using the corresponding vertical values.

Although for benzil (Table 5.2) and benzophenone compounds (Table 5.3), the lowest ionization potential corresponds to the highest Φ, there is no obvious general trend in the data in Fig. 6.2a. However, a good correlation between Φ and EA_a was found and is visualized using a second order polynomial fit in Fig. 6.2b. In Fig. 6.2c the corresponding plot for E_{HOMO}-E_{LUMO} is shown and it is seen that a small band gap has a less pronounced correlation with high Φ. A linear fit is used to show the general trend. The benzil-type voltage stabilizers substituted with alkyl chains were omitted here since the alkyl chains have a very small influence on the molecular energy levels but still seem to affect the molal stabilizing efficiency. Triazine1 and triazine2 were included despite having alkyl chain moieties with the reasoning that the alkyl chains should not be able to *decrease* the tree initiation field of the material compared to reference XLPE which is the case here. This is likely an electronic effect instead. DPPD was excluded since it at least partially degraded (as indicated by color change) during cross-linking. However, it would also have followed the trend in Fig. 6.2b with calculated EA_a of about -0.1 and Φ ~9 kg mol^{-1}.A wide range of voltage stabilizers were characterized in this way using previously reported data on electrical tree initiation from several different researchers as shown using grey diamonds in Fig. 6.2. Fullerenes are included using experimentally obtained IP, EA and E_{HOMO}-E_{LUMO} (*cf.* Table 6.2). For this data sets, substantial scattering is seen for Φ. This is to large extent caused by the non-linear concentration dependence of voltage stabilizers. In Fig. 6.2b for example, most outliers that give higher Φ than predicted by the fitted line is tested at a lower concentration, e.g. anthracene, PCBM and C_{60} are tested at 1 mmol kg^{-1}. Anthracene gives the predicted result following the trend in EA when tested at 10 mmol kg^{-1}.

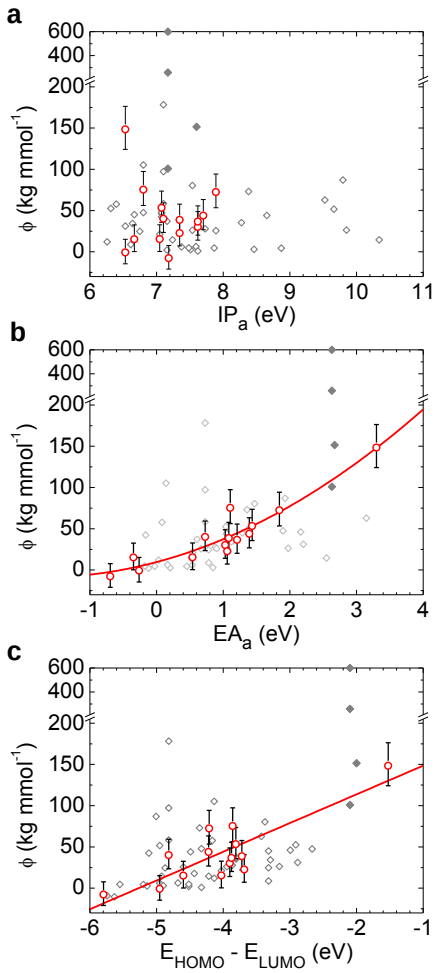

Figure 6.2. ***(a)*** *Adiabatic ionization potential IP_a,* ***(b)*** *adiabatic electron affinity EA_a and* ***(c)*** *E_{HOMO}-E_{LUMO} plotted against voltage stabilizing efficiency Φ. Red circles indicate that electrical treeing tests have been performed using the same test object geometry, stabilizer concentration (10 mmol kg^{-1}) and electrical test method as described in Chapter 4 of this thesis. The red lines are empirical fits to the red data points (2^{nd} order polynomial in* ***b*** *and linear in* ***c****. C_{60} fullerene and PCBM are included using experimental values for IP, EA and E_{HOMO}-E_{LUMO} (cf. Table 6.2) as indicated using filled grey diamonds. Energy levels for all other molecules were calculated using DFT B3LYP-6311+G(d,p). Φ was calculated for a wide selection of molecules and correlated with electrical tree initiation data from the literature references 22,23,84,86,87,93,103-108 (cf. Paper VI) and are plotted using grey diamonds.*

Table 6.1. *Calculated molecular properties using DFT b3lyp/6311+G(d,p) for a selection of the investigated voltage stabilizers. Adiabatic and vertical ionization potentials IP_a and IP_v, adiabatic and vertical electron affinities EA_a and EA_v as well as frontier orbital energies E_{HOMO} and E_{LUMO} are given in eV.*

	Voltage Stabilizer	IP_a	IP_v	EA_a	EA_v	E_{HOMO}	E_{LUMO}
Benzils	Et_1	7.71	7.83	1.40	0.92	-6.46	-2.24
	Es_2	8.02	8.25	1.75	1.41	-6.82	-2.61
	Am_1	6.82	6.83	1.13	0.62	-5.63	-1.77
Thioxanthones	ITX*	7.56	7.61	0.95	0.85	-6.11	-2.21
	MeOTX	7.34	7.45	0.96	0.82	-5.91	-2.22
	HOTX	7.49	7.59	1.00	0.86	-6.01	-2.28
	OTXAc	8.02	8.25	1.75	1.41	-6.82	-2.61
	OTXMa	7.21	7.81	1.33	1.26	-6.31	-2.50
Additional Compounds	Anthracene	7.11	7.18	0.72	0.62	-5.55	-2.01
	DOABP**	7.05	7.14	0.52	0.36	-5.63	-1.61
	Triazine 1**	7.18	7.19	-0.69	-0.70	-5.85	-0.05
	Triazine 2**	6.49	n.c.	-0.21	n.c.	-5.52	-0.57
	MPT	6.66	6.94	-0.37	-0.46	-5.35	-0.76
	DTDCPB	6.42	6.62	3.44	2.94	-5.61	-4.08

*Geometry with the isopropyl group in position 2 used for calculations
**Calculations were performed on corresponding systems where the octyl chains were replaced with ethylene groups.
n.c: not converged

Table 6.2. *Experimental ionization potential (IP_{exp}), electron affinity (EA_{exp}) and E_{HOMO}-E_{LUMO} in eV for C_{60} and PCBM.*

Voltage Stabilizer	**IP_{exp}**	**EA_{exp}**	**E_{HOMO}-E_{LUMO}**
C_{60}	7.6[109]	2.67[110]	-2.0[111]
PCBM	7.17[111]	2.63[112]	-2.1[111]

6.2 Voltage stabilizing mechanisms

The initiation of an electrical tree in a void-free material requires the formation of a micro-void large enough to sustain partial discharges. Electrons that have been accelerated in the electric field cause first impact excitation and at higher energies, impact ionization leading eventually to polymer chain scission (*cf.* mechanism in Fig. 6.3a). A voltage stabilizer acts by reducing the electron energy, preferably keeping it below the threshold energy for impact excitation of the polymer matrix. A.C. Ashcraft et al.[22] proposed two mechanisms relevant for voltage stabilization based on a series of polycyclic aromatic compounds. The first was that the voltage stabilizer would be ionized more easily compared to the polyethylene and thus protect the polyethylene from degradation. The secondary electrons produced when ionizing the voltage stabilizer have lower energy compared to the secondary electrons produced by ionizing the polyethylene and are therefore less likely to cause additional ionization (*cf.* Fig. 6.3b). The voltage stabilizer cation radical can then combine with another electron to regenerate the neutral species. The energy of the field-accelerated (hot) electrons needed for the onset of this mechanism is directly related to the ionization potential of the voltage stabilizer which is typically ~6-8 eV (*cf.* Fig 6.2a). The second means of interaction proposed by Ashcraft et al. is a mechanism where radicals on the polymer chain are quenched by direct electron transfer from a nearby voltage stabilizer molecule as can be seen in Fig. 6.3a. Zhang et al. propose the contribution of an impact excitation mechanism where energy from hot electrons is transferred to the voltage stabilizer which is excited and typically follows a phosphorescent pathway to relaxation, at least for acetophenone (*cf.* Fig. 6.3c).[113] The luminescence from voltage stabilizers was

observed by Yamano et al.[93] This mechanism can become active at lower electron energies and is related to the E_{HOMO}-E_{LUMO} difference, typically ~3-6 eV (*cf.* Fig. 6.2c). The correlation with electron affinity for the evaluated data set, as seen in Fig. 6.2b suggests an electron scavenging mechanism (*cf.* Fig. 6.3d). Similar trends have been found for the breakdown of polyethylene films as reported by Yamano et al.[114] as well as by Kisin et al.[115] Effective voltage stabilizers typically have adiabatic electron affinities of ~0.5-3.5 eV (*cf.* Fig. 6.2b) which in this case is the energy *gained* by the system when the stabilizer binds a free electron. This mechanism can thus be expected to be active as soon as electrons are injected into the dielectric. The electron energy required for the onset of the mechanisms presented in Fig. 6.3 increases in the order d-c-b-a as discussed above and before the initiation of treeing it can be expected that hot electrons reach sufficient energy for the onset of all four mechanisms.

Yamano et al. also suggest a void- filling mechanism which would require some degree of phase separation.[114] Yet, when concentration is increased above ~1.5wt% the performance gradually decreases until a tree initiation voltage below that of PE is observed caused by the field enhancing properties of larger stabilizer crystals. In the case of Et_{12}, as discussed in Chapter 5, it seems that field enhancing crystals are not formed even at high concentrations where the precipitation of stabilizer is clearly visible. Instead the performance remains rather constant at the maximum solubility limit.

It has also been proposed that the voltage stabilizers have a field grading effect.[26,116] At high voltage, the non-uniform field enhancement around a defect would attract the polarizable voltage stabilizer molecules by dielectrophoresis and cause enrichment of stabilizer around the defect. This would locally increase the permittivity of the dielectric around the defect and thus decrease the electric field strength. It seems unlikely that field grading would be solely responsible for the voltage stabilizing properties reported here but dielectrophoresis on the other hand could explain some of the observations within this thesis. In Paper II we see for example that a slow voltage ramp speed gives a slightly more pronounced effect of

the tested voltage stabilizer and in Paper III we see that increasing alkyl chain length from 1 to 12 and finally 30 carbons decreases the molar voltage stabilizer efficiency for the same type of system. Both observations could be related to diffusion of the stabilizer through the polyethylene matrix.

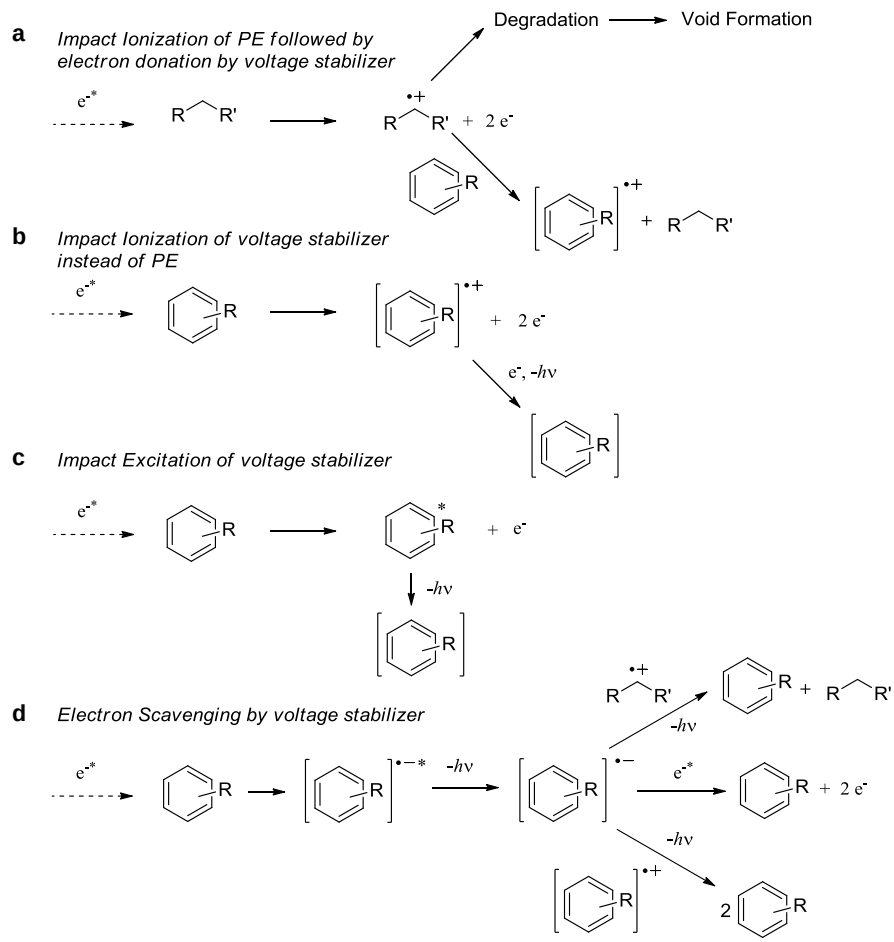

Figure 6.3. *Voltage stabilizing mechanisms.*

7 CONCLUDING REMARKS

The main focus of this thesis was to give further insight on the mechanisms of voltage stabilization. Through the testing of new stabilizers in conjunction with molecular modeling of electronic properties it was found that the electron affinity of a voltage stabilizer generally correlates with its stabilizing efficiency. This indicates that electron scavenging is a dominant mechanism for many voltage stabilizers. A similar but less pronounced correlation was found with the band gap, indicating that an impact excitation mechanism is likely to contribute to the voltage stabilizing effect. This is corroborated by a correlation between stabilizing effect and short triplet life times as observed for thioxanthone-type voltage stabilizers. However, it is also known that the triplet state lifetime is generally decreased by substitution with electron withdrawing groups[117] and it is therefore in this case difficult to distinguish whether an electron scavenging mechanism or an impact excitation mechanism is dominant. No correlation with ionization potential was found when expanding the data set outside specific groups of molecules, such as rigid aromatics or benzophenones as have been previously reported.[118]

Thorough analysis of the polymer microstructure using DSC and SAXS confirms that the voltage stabilizing effect is not caused by changes in polyethylene microstructure. In addition, the majority of the stabilizers presented in this thesis do not affect the gel content of the XLPE significantly at the tested concentration. However, fullerene containing samples exhibited increased gel content, a promising feature that indicates covalent bonding of the stabilizer preventing its migration.

A test method for efficient and accurate electrical treeing tests was developed, building on the previous work of Englund and Huuva.[77] The test objects were modified so that the wire loop was long enough to suppress the field reducing effect of the attachment point, in the previous case a semiconducting tab. It was shown that many trees initiate independently from each other, providing several data points from each test object. Additionally it was shown that more reliable results were

obtained using low ac ramp speed. The test method allows for high resolution microscopic observation as well as detection of partial discharge events.

Several voltage stabilizers were developed during the course of this project that were both efficient and compatible with common manufacture practice and an improvement of >100% at 0.33wt% addition was achieved for Es_2 after a period of annealing at room temperature. It was found that the introduction of long alkyl chains (C_{12} or C_{30}) decreases the efficiency of benzil voltage stabilizers. Although alkyl chains might be necessary to achieve compatibility for many material systems, it seems that they should not be made longer than necessary for solubilizing the stabilizer. An alternative is to use branched alkyl chains to hinder crystallization of the stabilizers. To widen the range of molecular electronic properties or to obtain reference points to compare with literature values, a few stabilizers were tested that either i) evaporated during degassing of peroxide by-products, ii) reacted with the peroxide during peroxide cross-linking or iii) had a too high melting point to be easily melt processed. An interesting find from these experiments was that fullerenes can be used as highly efficient voltage stabilizers even after reaction during the cross-linking. It was found that they can bind covalently to the polymer matrix and actually increase the gel content of the XLPE. The strongest improvement in the electrical tree initiation field (~148%) at 10 mmol kg^{-1} was found for a small-band gap material designed for organic solar cells. This material unfortunately have high melting point and degrades during cross-linking. It is, important to realize that for a substance with voltage stabilizing effect to be used as a voltage stabilizer in modern cable insulation it should not impair the insulation performance in any regard or pose a safety risk for operators during cable production.

ACKNOWLEDGEMENTS

I want to acknowledge the following people for their contributions to this thesis work.

Professor **Mats Andersson** for taking me on as a PhD student and for all the support and encouragement during this project.

My twin-PhD colleague **Anette Johansson**, professor **Stanislaw Gubanski** and **Jörgen Blennow** for all the help with high voltage measurements. Thanks also to **Thomas Hammarström** for well needed coffee and technical support.

Christian Müller for fantastic supervision during the later part of this project. Thank you for teaching me how to write manuscripts and for your constant optimism.

Villgot Englund for sharing your experiences and for always taking time to discuss my projects with me. Thank you also for all the help in your role as contact person with Borealis.

Angelica Lundin for teaching me about DFT modeling.

Harald Wutzel for all your input to this project, including synthesis and analysis work, co-supervision, and good company that you provided during your time here. Thanks also to **Wenjun Sun**, **Mattias Andersson** and **Jonas M. Bjuggren** for your contributions as project workers in relation to this project.

My students: **Jonas M. Bjuggren**, **Mattias Andersson**, **Espen Doedens**, **Adam Benson**, **Anna Rosell**, **Hanna Andersson**, **Henrik Sjövold**, **Johan Eklund**, **Nadia Serey**, **Oscar Hällqvist**, **Linus Kronlund** and **Patric Kvist** for the improved understanding we have gained from the results of you bachelor/master thesis works on voltage stabilizers or electrical treeing.

Frida Andersson, **Carina Pettersson**, **Christina Meyer**, **Anne Wendel**, **Ann Jacobsson**, **Kicki Stensvik**, **Lotta Pettersson Anders Mårtensson** and **Roger Forsman**, thanks for all your support and for making everything run smoothly at Applied Chemistry.

Arne Holmström for reading all my texts with enthusiasm and for your good feedback.

Timothy Steckler and **Renee Kroon** for all your help with organic synthesis

All my colleagues at floor 8, thank you for creating a fantastic environment for doing my PhD work. Special thanks to **Camilla Lindqvist**, **Mattias Andersson** and **Zandra George** for being such good friends and for reminding me to take coffee breaks.

My parents for the support during all years and for believing in me.

And finally, Katarina, I wouldn't have made it without you.

REFERENCES

1 Long, W. and Nilsson, S. *Power Energy Mag., IEEE*, **2007**, 5, 22-31
2 Flourentzou, N., Agelidis, V. G. and Demetriades, G. D. *Power Electron., IEEE Trans.*, **2009**, 24, 592-602
3 Worzyk, T. *Submarine Power Cables*; Springer Berlin Heidelberg, **2009**
4 Benato, R. B. and Paolucci, A. *Ehv Ac Undergrounding Electrical Power*; Springer London, **2010**
5 Capros, P., De Vita, A., Tasios, N., Papadopoulos, D., Siskos, P., Apostolaki, E., Zampara, M., Paroussos, L., Fragiadakis, K. and Kouvaritakis, N.; European Commision: Luxemburg: Publications Office of the European Union, **2013**
6 World Energy Outlook 2011; International Energy Agency (IEA), **2011**
7 *Smart Power Grids 2011*; Keyhani, A. and Marwali, M., Eds.; Springer Berlin Heidelberg, **2012**
8 Lua, X., McElroya, M. B. and Kiviluomac, J. *Proc. Natl. Acad. Sci. U. S. A.*, **2009**
9 Lenzen, M. and Baboulet, O. *Wind Energy* In *Handbook of Climate Change Mitigation*; Chen, W.-Y., Seiner, J., Suzuki, T. and Lackner, M., Eds.; Springer US, **2012**, 1295-1324
10 Lewis, N. S. and Nocera, D. G. *Proc. Natl. Acad. Sci. U. S. A.*, **2006**, 103, 15729-15735
11 Lee, S., Vandiver, M., Viswanathan, B. and Subramanian, V. *Harvesting Solar Energy Using Inexpensive and Benign Materials* In *Handbook of Climate Change Mitigation*; Chen, W.-Y., Seiner, J., Suzuki, T. and Lackner, M., Eds.; Springer US, **2012**, 1217-1261
12 Krothapalli, A. and Greska, B. *Solar Concentrators* In *Handbook of Climate Change Mitigation*; Chen, W.-Y., Seiner, J., Suzuki, T. and Lackner, M., Eds.; Springer US, **2012**, 1263-1294
13 Jia, J., Punys, P. and Ma, J. *Hydropower* In *Handbook of Climate Change Mitigation*; Chen, W.-Y., Seiner, J., Suzuki, T. and Lackner, M., Eds.; Springer US, **2012**, 1355-1401
14 Muraoka, H. *Geothermal Energy* In *Handbook of Climate Change Mitigation*; Chen, W.-Y., Seiner, J., Suzuki, T. and Lackner, M., Eds.; Springer US, **2012**, 1325-1353
15 European Commision, **2014**
16 The Ten-Year Network Development Plan and Regional Investment Plans; European Network of Transmission System Operators for Electricity (ENTSOE), **2012**
17 Seifi, H. and Sepasian, M. S. *Electric Power System Planning*; Springer Berlin Heidelberg, **2011**
18 Mazzanti, G. and Marzinotto, M., Eds. *Fundamentals of Hvdc Cable Transmission*; John Wiley & Sons, Inc., **2013**
19 Yan, P., Zhou, Y. and Yoshimura, N. *Proc. Inst. Electrostat. Jpn.*, **1999**, 23, 319-324

20 Zhou, Y., Wang, X., Yan, P., Liang, X., Guan, Z. and Yoshimura, N. *Electrical Insulation and Dielectric Phenomena, 2001 Annual Report. Conference on*, **2001**, 241-244

21 Boström, J. O., Marsden, E., Hampton, R. N. and Nilsson, U. *IEEE Elect. Insul. Mag. ,* **2003**, 19, 6-12

22 Ashcraft, A. C., Eichhorn, R. M. and Shaw, R. G. IEEE Int. Symp. Electr. Insul., **1976**, 213-218

23 Englund, V., Huuva, R., Gubanski, S. M. and Hjertberg, T. *Polym. Degrad. Stab.*, **2009**, 94, 823-833

24 Kiessling, F., Nefzger, P., Nolasco, J. F. and Kaintzyk, U. *Overhead Power Lines*; Springer Berlin Heidelberg, **2003**

25 Mazzanti, G. and Marzinotto, M., Eds. *Main Principles of Hvdc Extruded Cable Design*; John Wiley & Sons, Inc., **2013**

26 Peschke, E. and Olshausen, R. v. *Cable Systems for High and Extra-High Voltage: Development, Manufacture, Testing, Installation and Operation of Cables and Their Accessories*; Publicis MCD verlag, **1999**

27 Wenyuan, L., Vaahedi, E. and Choudhury, P. *Power Energy Mag., IEEE*, **2006**, 4, 52-58

28 Offshore Transmission Technology; European Network of Transmission System Operators for Electricity (ENTSOE), **2012**

29 Dixon, J., Moran, L., Rodriguez, J. and Domke, R. *Proc. IEEE*, **2005**, 93, 2144-2164

30 Jorge, R. S. and Hertwich, E. G. *Energy*, **2014**, 69, 760-768

31 Mehmet, D. *The History of Polyethylene* In *100+ Years of Plastics Leo Baekeland and Beyond*; American Chemical Society, **2011**, 115-145

32 Plastics-the Facts; Plastics Europe, **2013**

33 Vaughan, A., Davis, D. S. and Hagadorn, J. R. *Industrial Catalysts for Alkene Polymerization* In *Polymer Science: A Comprehensive Reference*; Matyjaszewski, K. and Möller, M., Eds.; Elsevier: Amsterdam, **2012**, 657-672

34 Kissin, Y. V. *Polyethylene - End-Use Properties and Their Physical Meaning*; Hanser Publishers, **2013**

35 Mark, H. F., Bikales, N. M., Overberger, C. G., Menges, G. and Kroschwitz, J. I., Eds. *Encyclopedia of Polymer Science and Engineering, Second Edition*; John Wiley & Sons, **1986**

36 Smedberg, A., Hjertberg, T. and Gustafsson, B. *Polymer*, **2004**, 45, 4867-4875

37 Ivanov, D. A. *Semicrystalline Polymers* In *Polymer Science: A Comprehensive Reference*; Matyjaszewski, K. and Möller, M., Eds.; Elsevier: Amsterdam, **2012**, 227-258

38 Gedde, U. W. *Polymer Physics*; Kluwer Academic Publishers, **1995**

39 Nilsson, S., Hjertberg, T. and Smedberg, A. *Europ. Polym. J.*, **2010**, 46, 1759-1769

40 Johnson, M. B., Wilkes, G. L., Sukhadia, A. M. and Rohlfing, D. C. *J. Appl. Pol. Sci.*, **2000**, 77, 2845-2864

41 Chu, B. and Hsiao, B. S. *Chemical Reviews*, **2001**, 101, 1727-1762

42 Glatter, O. and Kratky, O., Eds. *Small Angle X-Ray Scattering*; Academic Press: London, **1982**

43 Mark, J. E. *Physical Properties of Polymers Handbook*; Springer New York, **2007**
44 Wunderlich, B. and Bauer, H. *Heat Capacity of Linear High Polymers*; Springer Verlag, **1970**
45 Bair, H. E., Huseby, T. W. and Salovey, R. *The Equilibrium Melting Temperature and Surface Free Energy of Polyethylene Single Crystals* In *Analytical Calorimetry*; Porter, R. and Johnson, J., Eds.; Springer US, **1968**, 31-40
46 Hoffman, J. D. and Lauritzen, J. I. *J. Res. Nat. Bur. Stand.*, **1961**, A 65, 297-336
47 Peacock, A. *Handbook of Polyethylene: Structures: Properties, and Applications*; CRC Press, **2000**
48 Moyses, S. C. and Zukermann-Schpector, J. *Polym. J.*, **2004**, 36, 679
49 Kröhnke, C. *Polymer Additives* In *Polymer Science: A Comprehensive Reference*; Matyjaszewski, K. and Möller, M., Eds.; Elsevier: Amsterdam, **2012**, 349-375
50 Zweifel, H. *Stabilization of Polymeric Materials*; Springer-Verlag, **1998**
51 Duval, M. and St-Onge, H. *Electr. Insul., IEEE Trans.*, **1979**, EI-14, 264-271
52 Nilsson, U. H., Dammert, R. C., Campus, A., Sneck, A. and Jakosuo-Jansson, H. Cond. Break. Sol. Dielectr., 1998. ICSD '98. Proc. IEEE 6th Int. Conf., 22-25 Jun 1998 **1998**, 365-367
53 Holmström, A. and Sörvik, E. M. *J. Appl. Pol. Sci.*, **1974**, 18, 761-778
54 Charlesby, A. and Pinner, S. H. *Proc. Roy. Soc. Lon. A, Math. Phys. Sci.*, **1959**, 249, 367-386
55 Lazár, M., Rado, R. and Rychlý, J. *Crosslinking of Polyolefins* In *Pol. Phys.*; Springer Berlin Heidelberg, **1990**, 149-197
56 Andrews, T., Hampton, R. N., Smedberg, A., Wald, D., Waschk, V. and Weissenberg, W. *IEEE Elect. Insul. Mag.*, **2006**, 22, 5-16
57 Hulse, G. E., Kersting, R. J. and Warfel, D. R. *J. Pol. Sci. A Pol. Chem.*, **1981**, 19, 655-667
58 Olejniczak, J., Rosiak, J. and Charlesby, A. *Rad. Phys. Chem.*, **1991**, 37, 499-504
59 Cartasegna, S. *Rubber Chem. Tech.*, **1986**, 59, 722-739
60 Palmlöf, M., Hjertberg, T. and Sultan, B. Å. *J. Appl. Pol. Sci.*, **1991**, 42, 1193-1203
61 Beveridge, C. and Sabiston, A. *Mater. Design*, **1987**, 8, 263-268
62 Smedberg, A., Hjertberg, T. and Gustafsson, B. *Polymer*, **1997**, 38, 4127-4138
63 Ross, R. *Dielectr. Electr. Insul., IEEE Trans.*, **1998**, 5, 660-680
64 Wright, D. C. *Environmental Stress Cracking of Plastics*; Smithers Rapra Technology, **1996**
65 Kitchin, D. W. and Pratt, O. S. *Electr. Eng.*, **1958**, 77, 218-223
66 Laurent, C. and Teyssedre, G. *Nucl. Instrum. Methods Phys. Res. B*, **2003**, 208, 442-447
67 Dissado, L. A. and Fothergill, J. C. *Electrical Degradation and Breakdown in Polymers*; Institution of Engineering and Technology, **1992**

68 Teyssedre, G. and Laurent, C. *J. Appl. Phys.*, **2008**, 103, 046107-046107-046102

69 Tanaka, T. *Electr. Insul., IEEE Trans.*, **1992**, 27, 424-431

70 Bruce, S. B. *Fundamentals of Electrical Insulation Materials*; CRC Press, **2011**

71 Doedens, E., Johansson, A., Jarvid, M., Nilsson, S., Bengtsson, M. and Kjellqvist, J. Electr. Insul. Dielectr. Phen. (CEIDP), 2012 Ann. Rep. Conf., 14-17 Oct. **2012**, 597-600

72 Wang, J.-f., Zheng, X.-q., Wu, J., Li, Y.-x. and Zhang, Z.-j. Prop. Appl. Dielectr. Mater. (ICPADM), 2012 IEEE 10th Int. Conf., 24-28 July **2012**, 1-6

73 Muto, H., Motohashi, K., Maruyama, Y. and Iwata, Z. Cond. Break. Sol. Diel., 1992., Proc. 4th Int. Conf., 22-25 Jun. **1992**, 461-469

74 Dissado, L. A. *Dielectr. Electr. Insul., IEEE Trans.*, **2002**, 9, 483-497

75 Yang, J. J. and Brilasekaran, S. Power Eng. Conf., 2005. IPEC 2005. 7th Int., Nov. 29 2005-Dec. 2 **2005**, 1-34

76 *IEEE Guide for the Statistical Analysis of Electrical Insulation Breakdown Data*, IEEE Standard 930-2004.

77 Huuva, R., Englund, V., Gubanski, S. M. and Hjertberg, T. *Dielectr. Electr. Insul., IEEE Trans.*, **2009**, 16, 171-178

78 Jarvid, E. M., Johansson, A. B., Blennow, J. H. M., Andersson, M. R. and Gubanski, S. M. *Dielectr. Electr. Insul., IEEE Trans.*, **2013**, 20, 1712-1719

79 Jarvid, M., Johansson, A., Englund, V., Gubanski, S. and Andersson, M. R. Electr. Insul. Dielectr. Phen. (CEIDP), 2012 Ann. Rep. Conf., 14-17 Oct. **2012**, 605-608

80 COMSOL Multiphysics® Version 4.2.; COMSOL, Inc. : Burlington, MA, USA., **2011**

81 *Standard Test Method for Evaluation of Resistance to Electrical Breakdown by Treeing in Solid Dielectric Materials Using Diverging Fields*; ASTM Standard D3756, 2007 (2010); ASTM International: West Conshohocken PA, **2007**

82 GB1083113(A); Simplex Wire & Cable CO, **1967**

83 GB1116398A; Simplex Wire & Cable CO, **1968**

84 Heidt, L. J. CA832524 (A); Simplex Wire & Cable CO, **1970**

85 Takahashi, M., Ito, A., Igarashi, Y., Kawada, S., Ogura, J. and Ito, R. US3933772; Kureha Chemical Ind. CO LTD, **1976**

86 Martinotto, L., Peruzzotti, F. and Del Brenna, M. US2002164480 (A1), **2002**

87 Englund, V., Huuva, R., Gubanski, S. M. and Hjertberg, T. *Dielectr. Electr. Insul., IEEE Trans.*, **2009**, 16, 1455-1461

88 Richards, K. E., McMaster, B. N. and Wright, G. J. *Org. Mass Spectrom.*, **1975**, 10, 295-312

89 Fouassier, J. *Photoinitiation, Photopolymerization and Photocuring*; Hanser Publishers, **1995**

90 Neumann, M., Gehlen, V., Encinas, M., Allen, N., Corrales, T., Peinado, C. and Catalina, F. *J. Chem. Soc., Far. Trans.*, **1997**, 93, 1517-1521

91 Kroto, H. W., Heath, J. R., Obrien, S. C., Curl, R. F. and Smalley, R. E. *Nature*, **1985**, 318, 162-163

92 Hirsch, A. and Brettreich, M. *Fullerenes: Chemistry and Reactions*; Wiley-VCH: Weinheim, **2006**
93 Yamano, Y. and Iizuka, M. *Dielectr. Electr. Insul., IEEE Trans.*, **2009**, 16, 189-198
94 Chen, Y.-H., Lin, L.-Y., Lu, C.-W., Lin, F., Huang, Z.-Y., Lin, H.-W., Wang, P.-H., Liu, Y.-H., Wong, K.-T., Wen, J., Miller, D. J. and Darling, S. B. *J. Am. Chem. Soc.*, **2012**, 134, 13616-13623
95 Patsch, R. *Electr. Insul., IEEE Trans.*, **1979**, EI-14, 200-206
96 Takahashi, T., Ohtsuka, H., Takehana, H. and Niwa, T. *Power App. Syst., IEEE Trans.* , **1985**, PAS-104, 1945-1950
97 Krusic, P. J., Wasserman, E., Keizer, P. N., Morton, J. R. and Preston, K. F. *Science*, **1991**, 254, 1183-1185
98 Brois, S. J., Patil, A. O., Schulz, W. W., Hsu, C. S. and Garner, R. T. US5462680 (A), **1995**
99 Frisch, M. J., Trucks, G. W., Schlegel, H. B., Scuseria, G. E., Robb, M. A., Cheeseman, J. R., Scalmani, G., Barone, V., Mennucci, B., Petersson, G. A., Nakatsuji, H., Caricato, M., Li, X., Hratchian, H. P., Izmaylov, A. F., Bloino, J., Zheng, G., Sonnenberg, J. L., Hada, M., Ehara, M., Toyota, K., Fukuda, R., Hasegawa, J., Ishida, M., Nakajima, T., Honda, Y., Kitao, O., Nakai, H., Vreven, T., Montgomery Jr., J. A., Peralta, J. E., Ogliaro, F., Bearpark, M. J., Heyd, J., Brothers, E. N., Kudin, K. N., Staroverov, V. N., Kobayashi, R., Normand, J., Raghavachari, K., Rendell, A. P., Burant, J. C., Iyengar, S. S., Tomasi, J., Cossi, M., Rega, N., Millam, N. J., Klene, M., Knox, J. E., Cross, J. B., Bakken, V., Adamo, C., Jaramillo, J., Gomperts, R., Stratmann, R. E., Yazyev, O., Austin, A. J., Cammi, R., Pomelli, C., Ochterski, J. W., Martin, R. L., Morokuma, K., Zakrzewski, V. G., Voth, G. A., Salvador, P., Dannenberg, J. J., Dapprich, S., Daniels, A. D., Farkas, Ö., Foresman, J. B., Ortiz, J. V., Cioslowski, J. and Fox, D. J.; Gaussian, Inc.: Wallingford, CT, USA, **2009**
100 Krishnan, R., Binkley, J. S., Seeger, R. and Pople, J. A. *J. Chem. Phys.*, **1980**, 72, 650-654
101 Becke, A. D. *J. Chem. Phys.*, **1993**, 98, 5648-5652
102 Lee, C., Yang, W. and Parr, R. G. *Phys. Rev. B*, **1988**, 37, 785-789
103 Jarvid, M., Johansson, A., Bjuggren, J. M., Wutzel, H., Englund, V., Gubanski, S., Müller, C. and Andersson, M. R. *J. Pol. Sci. B Pol. Phys.*, **2014**, 52, 1047-1054
104 Jarvid, M., Johansson, A., Kroon, R., M. Bjuggren, J., Wutzel, H., Englund, V., Gubanski, S., Andersson, M. R. and Müller, C. *Manuscript*, **2014**
105 Wutzel, H., Jarvid, M., M. Bjuggren, J., Johansson, A., Englund, V., Gubanski, S. and Andersson, M. R. *submitted pol. deg. stab.*, **2014**
106 Kato, H. and Maekawa, N. US3956420 (A); Dainichi Nippon Cables LTD, **1976**
107 Davis, H. J. US4216101 (A); Canada Wire & Cable CO, **1980**
108 Person, T. J. and Cogen, J. M. WO2012050792 (A1), **2012**
109 Yoo, R. K., Ruscic, B. and Berkowitz, J. *J. Chem. Phys.*, **1992**, 96, 911-918
110 Brink, C., Andersen, L. H., Hvelplund, P., Mathur, D. and Voldstad, J. D. *Chemical Physics Letters*, **1995**, 233, 52-56

111 Akaike, K., Kanai, K., Yoshida, H., Tsutsumi, J. y., Nishi, T., Sato, N., Ouchi, Y. and Seki, K. *J. Appl. Phys.*, **2008**, 104, 023710
112 Larson, B. W., Whitaker, J. B., Wang, X.-B., Popov, A. A., Rumbles, G., Kopidakis, N., Strauss, S. H. and Boltalina, O. V. *J. Phys. Chem. C*, **2013**, 117, 14958-14964
113 Fang, W.-H. and Phillips, D. L. *ChemPhysChem*, **2002**, 3, 889-892
114 Yamano, Y. *Dielectr. Electr. Insul., IEEE Trans.*, **2006**, 13, 773-781
115 Kisin, S., den Doelder, J., Eaton, R. F. and Caronia, P. J. *Pol. Deg. Stab.*, **2009**, 94, 171-175
116 Feichtmayr, F. and Wuerstlin, F. *Kunstst.*, **1970**, 60, 381-385
117 Encinas, M. V., Rufs, A. M., Corrales, T., Catalina, F., Peinado, C., Schmith, K., Neumann, M. G. and Allen, N. S. *Polymer*, **2002**, 43, 3909-3913
118 Englund, V. and Hjertberg, T. Jicable 2011, Versailles, France, **2011**